

A hybrid additive and subtractive manufacturing approach for multi-material components

by

Eric Weflen

A thesis submitted to the graduate faculty

in partial fulfillment of the requirements for the degree of

MASTER OF SCIENCE

Major: Industrial Engineering

Program of Study Committee:

Matthew C. Frank, Major Professor

Peter Collins

Frank Peters

The student author, whose presentation of the scholarship herein was approved by the program of study committee, is solely responsible for the content of this. The Graduate College will ensure this thesis is globally accessible and will not permit alterations after a degree is conferred.

Iowa State University

Ames, Iowa

2020

Copyright © Eric Weflen, 2020. All rights reserved.

DEDICATION

I dedicate this thesis to my parents, who support me unconditionally.

TABLE OF CONTENTS

	Page
LIST OF FIGURES	iv
LIST OF TABLES	vi
NOMENCLATURE	vii
ACKNOWLEDGMENTS	viii
ABSTRACT.....	ix
CHAPTER 1. GENERAL INTRODUCTION	1
1.1 Background	1
1.1.1 Subtractive and Additive Manufacturing	2
1.1.2 Hybrid Manufacturing	4
1.2 Research Problem	7
1.3 Research Objectives.....	8
1.4 Thesis Organization	9
1.5 References	9
CHAPTER 2. LITERATURE REVIEW	11
2.1 Additive Manufacturing on a Large Scale	11
2.2 Hybrid Additive and Subtractive Manufacturing.....	13
2.3 Multiple Material Components	15
2.4 References	17
CHAPTER 3. MECHANICAL ROOT STRUCTURE FOR MULTI-MATERIAL HYBRID ADDITIVE AND SUBTRACTIVE MANUFACTURING	21
3.1 Abstract	21
3.2 Introduction	22
3.3 Related Work	24
3.4 Solution Overview	26
3.5 Effect of Process Parameters and Cooling	28
3.6 The development of a Mechanical Dovetail Joint	36
3.7 Conclusions	42
3.8 References	43
CHAPTER 4. GENERAL CONCLUSIONS.....	47

LIST OF FIGURES

	Page
Figure 1.1 Formative, subtractive, and additive manufacturing processes (Redwood <i>et al.</i> , 2017).....	1
Figure 1.2 Layer-based approximation of geometry in additive manufacturing.	4
Figure 1.3 An additive process balances productivity and surface finish while hybrid achieves both (Jones, 2014).....	5
Figure 1.4 A hybrid hydroforming-injection molding metal-polymer component from the Tesla Model Y (Munro Live 2020).	6
Figure 1.5 Mechanically interlocking root structure for metal-polymer components.	8
Figure 2.1 The effect layer thickness has on the ability to reproduce a surface geometry (Chesser <i>et al.</i> , 2019).....	11
Figure 2.2 A comparison between (a) FFF and (b) BAAM, which uses a screw extruder (Chesser <i>et al.</i> , 2019; Turner <i>et al.</i> , 2014).....	12
Figure 2.3 Shape Deposition Manufacturing of heterogeneous objects (Weiss <i>et al.</i> , 1997).....	13
Figure 2.4 Comparison between characteristics of CNC machining and AM (Hur <i>et al.</i> , 2002).....	14
Figure 2.5 Rigid polymer component with an overmolded flexible gasket (Protolabs, 2018).....	15
Figure 2.6 Mechanical interlocks used in multi-material injection molded components (GLS Corporation, 2004).	16
Figure 3.1 Extruded polymer fails to adhere to a clean aluminum surface.	23
Figure 3.2 Mechanical interlocking features retain gas turbine blades (Combined Cycle Journal, 2012).	23
Figure 3.3 The process for creating a mechanical root structure in the material interface.....	26
Figure 3.4 a) Open-ended versus b) closed-loop contour for dovetail feature.	27
Figure 3.5 Metal-polymer multi-material component. a) Machined aluminum region with root features in the interface. b) Aluminum and ABS/CF multi-material component. c) Cross-section exposing the material interface.	27

Figure 3.6 Simulated tool paths from the ORNL slicer and the resulting part.	28
Figure 3.7 Results of 30 second layer time overhang test. a) 55° overhang collapse b) z-seam defects c) supported overhang comparison	30
Figure 3.8 Un-anchored overhang test samples with 30, 60, 120, 180 second minimum layer time enforced by pausing at the end of each layer.	31
Figure 3.9 Four tensile bars are waterjet cut from each 3D printed slab then machined.....	32
Figure 3.10 Porosity found in samples.	33
Figure 3.11 Tensile bar slab produced with a spindle speed of 120 rpm has material squeezing upward, a sign of over extrusion.	33
Figure 3.12 Slumping seen in section of printed part with 30s layer times.....	34
Figure 3.13 Fracture surface of a tensile test bar.	34
Figure 3.14 Interlayer strength of deposited carbon fiber reinforced ABS along the z-axis of the part. Error bars represent standard error of the mean using four test samples, except for the 110 rpm, 30 second layer time and 120 rpm, 180 second layer time sample sets which only contain three samples and the 110 rpm, 60 second layer time sample set that only contains two samples.	35
Figure 3.15 A-B) Circular toolpath for the dovetail profile. C-D) A concave-convex toolpath for the dovetail profile.	36
Figure 3.16 Tensile sample is produced by a) machining the dovetail profile in aluminum b) extruding ABS/CF c) machining the printed material.....	37
Figure 3.17 a) Dovetail profile is underfilled with polymer b) Dovetail profile with complete fill.....	38
Figure 3.18 Tensile test setup for the mechanical interlocking root.....	39
Figure 3.19 Tensile strength of the joint between machined aluminum and extruded ABS/CF normalized by the cross-section of the machined dovetail feature.....	40
Figure 3.20 Typical tensile test failure for circular and concave-convex root structures.....	40
Figure 3.21 Bulk 3D printed ABS/CF failure of tensile test samples.....	41

LIST OF TABLES

	Page
Table 3.1 Process parameters used in the ORNL Slicer for use with the AMBIT PE-1 tool in a HAAS UMC750 mill.....	29
Table 3.2 Process parameters used for tensile test samples. Samples that failed outside of the neck region or were damaged during preparation are excluded.	32

NOMENCLATURE

ABS	Acrylonitrile butadiene styrene
ABS/CF	ABS with Carbon Fiber Reinforcement
AM	Additive Manufacturing
BAAM	Big Area Additive Manufacturing
CAD	Computer Aided Design
CAM	Computer Aided Manufacturing
CNC	Computer Numerical Control
DED	Directed Energy Deposition
FDM	Fused Deposition Modeling
FFF	Fused Filament Fabrication
HM	Hybrid Manufacturing
LSAM	Large Scale Additive Manufacturing
ME	Material Extrusion
SDM	Shape Deposition Modeling

ACKNOWLEDGMENTS

I would like to thank my committee chair, Matt Frank, and my committee members, Frank Peters, and Peter Collins, for their guidance and support throughout the course of this research.

In addition, I would also like to thank my friends, colleagues, the department faculty and staff for making my time at Iowa State University a wonderful experience. I want to also offer my appreciation to those who helped support my research, especially Aaron Jordan, without whom this thesis would not have been possible.

ABSTRACT

This research introduces a hybrid additive and subtractive method for producing multiple material components consisting of metal and polymer regions. The method expands the notion of hybrid beyond multiple processes, to include multi-materials, taking advantages from each process and material. An AMBIT PE-1 polymer screw extrusion tool has been integrated into a HAAS machining center, bringing large scale additive manufacturing in-envelope with subtractive manufacturing. In this thesis, the effect of cooling time on the ability to reproduce overhanging geometry and on the strength of the interlayer bonding is investigated. This evaluation provides the baseline needed to evaluate the strength of the material transition. A mechanically interlocking root structure is developed to join regions of dissimilar materials into a single component. Two geometries of this root structure are evaluated for their mechanical strength. This method of creating a mechanical bond between substrates can be applied in hybrid additive and subtractive applications where dissimilar materials have limited chemical compatibility. Expanding the material capabilities of hybrid manufacturing enables a future of rapid manufacturing where a wide range of complex components can be produced on a single piece of hardware without the need for part-specific tooling.

CHAPTER 1. GENERAL INTRODUCTION

1.1 Background

Manufacturing processes can be categorized as formative, subtractive, or additive (Figure 1.1). Each category has its own set of advantages, constraints, and disadvantages. Formative processes, such as injection molding or forging, start with bulk material and shape it into its final form. Machining (milling, turning, grinding) is a subtractive manufacturing process that also starts with a bulk material; however, the material is removed from the part until the final geometry is attained. While this has the advantage of not requiring the expensive tooling needed

for many forming operations, machining requires the cutting tool to have visibility to the material being removed; making undercuts difficult or impossible. Additive Manufacturing (AM), selectively deposits material as needed in a layer-by-layer approach until the final geometry is realized. AM allows for complex geometries and

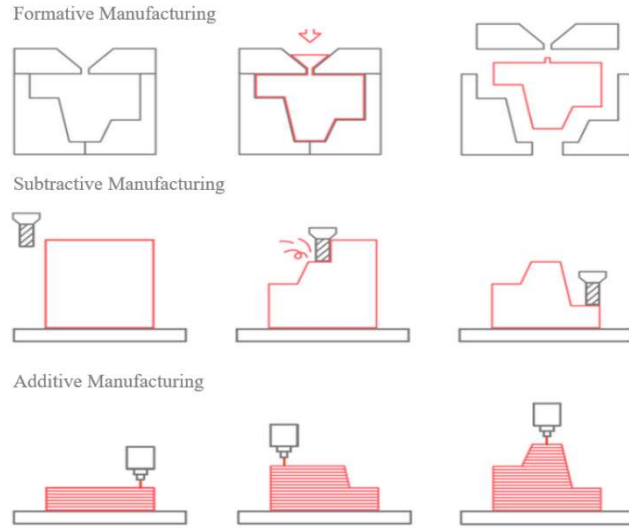


Figure 1.1 Formative, subtractive, and additive manufacturing processes (Redwood *et al.*, 2017).

internal features to be produced, but it is generally a slow process due to its inherent tradeoff between surface roughness and productivity. The cost, quality, and design of a component is driven by the capabilities of its manufacturing process, making the alignment between its functional requirements and the chosen process critical.

To better meet the functional requirements of a part, multiple manufacturing processes can be combined, creating a Hybrid Manufacturing (HM) process. These HM techniques can

avoid the weaknesses while taking advantage of the strengths of each process, creating a new process with capabilities beyond those of each individual process. A common HM pairing has been AM and subtractive manufacturing, which allows for thick layers of material to be deposited and the surface selectively machined to meet surface roughness or dimensional requirements. Hybridization is not limited to the manufacturing processes but can also be extended to the material composition. These multiple material components can more effectively meet functional requirements, such as wear resistance, strength, or weight through localized material selection. By combining materials with drastically different properties, like metals and polymers, a single part can meet both strength and weight targets that a homogenous part could not achieve. However, due to different processing parameters needed for dissimilar materials, such as melting temperature, there is not a clear solution for producing hybrid metal-polymer components in a hybrid additive and subtractive manufacturing system. The following sections provide an overview of subtractive and additive manufacturing, hybrid manufacturing.

1.1.1 Subtractive and Additive Manufacturing

Machining and other subtractive manufacturing processes have a long history in industry. The removal of material to achieve the final shape allows for the production of parts with accurate dimensions and fine surface finishes. Machining processes have been automated using Computer Numerical Control (CNC), improving the geometry that can be produced while also improving productivity (Zhang *et al.*, 2011). Since subtractive processes start with a stock of material and cut it to shape, they have the potential to quickly produce large objects. However, this requires the starting stock of material to be large enough to contain all the part geometry, which may lead to excessive material removal, waste, and long processing times. It also typically means the entire part is comprised of a single material. This challenge can be partially overcome

by creating a near-net-shape part in a formative process such as casting or injection molding, then machining the areas where more accurate dimensions or better surface finish are required. Still, this combination of processes involves the expensive tooling needed for formative manufacturing and again typically limits the component to a single material. Subtractive processes also require that the cutting tool has access to the material desired to be removed, making undercuts a challenge and internal geometry impossible.

In 1984 a patent was filed by Charles Hull for an automated additive manufacturing process, where a 3D part could be produced by selectively adding layers of material (Hull *et al.*, 1984). This invention, referred to as Stereolithography, launched the additive manufacturing market and field of research. AM allows for the free-form production of parts without expensive tooling and with automated process planning. It also enables the fabrication of new geometries, such as lattice structures or internal features, due to its layer-based production process. Similar to most manufacturing processes, AM has tradeoffs that can limit its application in industry. Additive manufacturing tends to be slower per part than other processes partially due to the tradeoff between productivity and surface roughness (layer thickness).

Over the past several decades, many different AM technologies have been invented. The standard ISO/ASTM 52900:2015 defines seven categories of AM, with one of the most common techniques being material extrusion (ME). In ME, the material is extruded through a nozzle in a layer by layer fashion to produce the desired geometry (Figure 1.2). While there are numerous ME techniques, fused deposition modeling (FDM), also known as fused filament fabrication (FFF), is prominent.

While FFF systems typically use polymer in the form of a filament, a more recent development has been larger-scale FFF systems using a screw extruder or gear pump to pressurize and extrude polymer from pellet feedstock. These systems, such as Cincinnati's Big Area Additive Manufacturing (BAAM), Thermwood's Large Scale Additive Manufacturing (LSAM), or Hybrid Technologies' AMBIT PE-1, can deposit material at a rate two orders of magnitude greater than most filament-based systems. The faster material flow rate allows for thicker layers, enabling the production of large parts

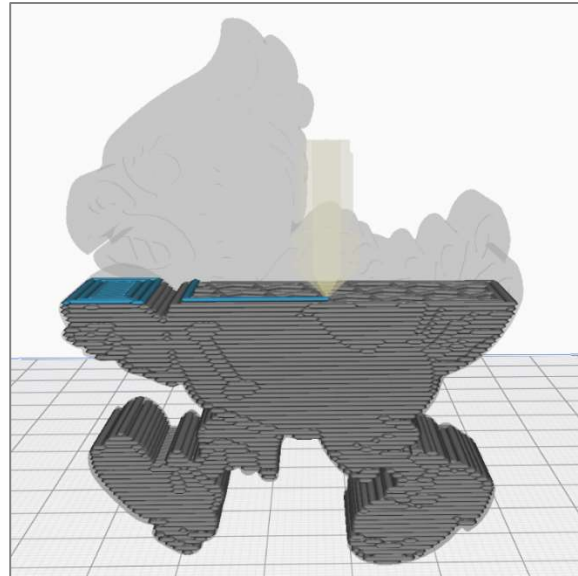


Figure 1.2 Layer-based approximation of geometry in additive manufacturing.

more quickly. However, the thick layers increase surface roughness and thus the error between the desired geometry and the part produced. The high stair step error has led to the hybridization of many large FFF systems with subtractive machining to achieve geometric accuracy and surface roughness requirements while maintaining gains in productivity.

1.1.2 Hybrid Manufacturing

Manufacturing processes can be combined, creating a hybrid manufacturing (HM) process. While there is debate over what constitutes an HM process, it has been proposed to be the combination of multiple processes into a single system resulting in capabilities greater than the two separate processes (Lauwers *et al.*, 2014; Zhu *et al.*, 2013). The strengths of each process are exploited while the weaknesses can be avoided, creating a synergistic effect where the new hybrid process is more capable than the sum of its parts (Jones, 2014). This combination can take

place in-envelope, i.e., in a single manufacturing cell, or out-of-envelope in a serial manner. In-envelope HM systems have the benefit of reducing the number of times the part needs to be fixtured and zeroed, allowing for streamlined processing. By decreasing the number of human interventions in the process, an in-envelope system can also reduce opportunities for error.

Components often have tight tolerances and strict surface finish requirements, which subtractive processes like machining can achieve. However, machining has limited capabilities in producing highly complex geometries, which is a strength of additive manufacturing. Unfortunately, metal additive manufacturing processes are not capable of maintaining as tight of tolerances or producing the surface finishes that machining can produce. To meet these requirement, there has been a race to produce thin layers that better reproduce the desired geometry, but again, this comes at the cost of processing time. If thick layers are used, the processing time drops precipitously, but it has a detrimental effect on the quality of the surface finish and the stair-step error. By hybridizing AM and subtractive machining, large parts can be produced quickly without sacrificing surface finish or dimensional accuracy (Figure 1.3).

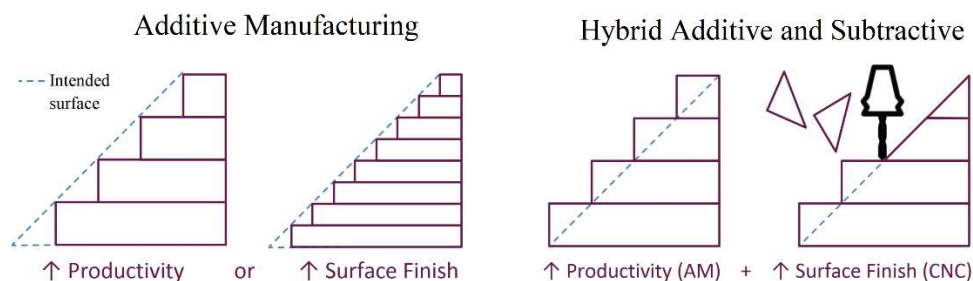


Figure 1.3 An additive process balances productivity and surface finish while hybrid achieves both (Jones, 2014).

The HM concept can be taken a step further and used to merge processing technologies for dissimilar materials not generally compatible with a single manufacturing process. These are materials with processing characteristics, such as melt temperature or chemical composition, that prevent them from being processed using similar parameters or techniques such as metals and polymers. Nevertheless, integrating materials with distinct properties into a single component can lead to efficiencies or capabilities not obtainable by homogenous objects. Since they allow for a higher degree of differentiation when optimizing the material to meet the functional requirements of each region of the part, a more significant improvement can be attained. Figure 1.4 shows an example of a multi-material hybrid process where hydroforming of aluminum and injection molding of a fiber-reinforced polymer are combined in-envelope to reduce weight and component count in automotive structures (Albert *et al.*, 2015).



Figure 1.4 A hybrid hydroforming-injection molding metal-polymer component from the Tesla Model Y (Munro Live 2020).

Material regions are specified using a digital part file divided into voxels, three-dimensional pixels, each with specified material properties. Digital material assignment and fabrication may have increasing importance in product design as smart assistants and automated

design tools become more prominent. For example, topology optimization or machine learning can be used to mimic structures found in nature to more effectively meet functional requirements specified by a design engineer (Hiller and Lipson, 2009). These systems can develop part designs that are more complex than an engineer could produce using current computer-aided design tools.

A challenge with multiple material components is that there are limited joining mechanisms for the interface, including mechanical, chemical, thermal (fusion or solid-state), or a combination of these methods (Martinsen *et al.*, 2015). In systems with dissimilar materials, the chemical and thermal properties are often too different for these types of bonds, leaving mechanical bonding as the only option. However, there is a lack of techniques for producing mechanical bonding in hybrid additive-subtractive manufacturing systems, which has prevented the development of metal-polymer components. Although fasteners can be used (e.g., screws, bolts, rivets, etc.), the complexity of assembly is not conducive to an automated, rapid manufacturing technology.

1.2 Research Problem

An in-envelope hybrid additive and subtractive system can produce parts more effectively than either stand-alone process, while multi-material parts comprised of metal and polymer regions can better meet functional requirements. Despite this, a method for producing metal-polymer components in such a hybrid system does not exist because a compatible joining technique is yet to be developed. To be effective, the inter-material joint must have strength similar to the bulk material, have geometric flexibility to work with a wide range of interface geometries, and require minimal operator interaction.

In this work, it is proposed that a feature with an undercut can be machined into the surface of the metal/polymer interface, into which polymer can be extruded. While molten, the polymer can form to the shape of the undercut profile, then lock in place as it cools, forming a mechanically interlocking root-like structure. A challenge with an undercut profile is that it does not constrain motion along the direction of the cut, so a simple straight path cannot be used if all degrees of freedom are to be fully constrained. Also, as the molten polymer undergoes a phase transformation, and as it continues cooling to room temperature, it will shrink. This could cause the locking mechanism to loosen and allow the root to move freely. The path that the cutting tool follows must be one that uses this shrinking action to create a tight interference fit as the molten polymer solidifies. A method of producing a mechanical root system is needed to expand the capabilities of HM to include metal-polymer components.

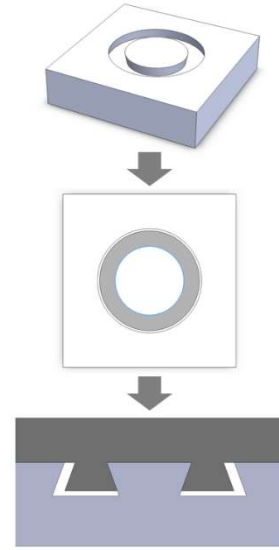


Figure 1.5 Mechanically interlocking root structure for metal-polymer components.

1.3 Research Objectives

The objective of this research is to develop an in-envelope hybrid manufacturing method for multi-material parts. More specifically, this work will create and evaluate a mechanical joining method needed to achieve automated hybrid manufacturing of metal-polymer components. This objective is achieved through three sub-objectives:

1. Measure the performance of carbon fiber/ABS material printed using a material extrusion system integrated into a machining center.
2. Develop a metal-polymer interface for hybrid additive and subtractive manufacturing.
3. Evaluate the mechanical performance of an aluminum – carbon fiber/ABS root structure.

1.4 Thesis Organization

The remainder of this thesis is organized as follows. Chapter 2 reviews state of the art in hybrid manufacturing of multiple material components. Chapter 3 presents a method for joining dissimilar materials in a hybrid manufacturing process and evaluates their performance. The conclusions are offered in chapter 4, along with opportunities for future research in this area.

1.5 References

- Albert, A., Drossel, W.G., Zorn, W., Nendel, W. and Raithel, D. (2015), "Process combination of hydroforming and injection moulding for the insitu manufacturing of metal and plastic composite structures", *Materials Science Forum*, available at: <https://doi.org/10.4028/www.scientific.net/MSF.825-826.522>.
- Hiller, J.D. and Lipson, H. (2009), "Multi material topological optimization of structures and mechanisms", *Proceedings of the 11th Annual Genetic and Evolutionary Computation Conference, GECCO-2009*, available at: <https://doi.org/10.1145/1569901.1570105>.
- Hull, C.W., (1984), "Apparatus for production of 3D objects by stereolithography", *United States Patent*.
- Jones, J.B. (2014), "The synergies of hybridizing CNC and additive manufacturing", *Technical Paper - Society of Manufacturing Engineers*.
- ISO/ASTM (2015), "ISO/ASTM 52900-2015: Additive Manufacturing - General Principles - Terminology", ISO/ASTM Standards.
- Lauwers, B., Klocke, F., Klink, A., Tekkaya, A.E., Neugebauer, R. and McIntosh, D. (2014), "Hybrid processes in manufacturing", *CIRP Annals - Manufacturing Technology*, available at: <https://doi.org/10.1016/j.cirp.2014.05.003>.
- Martinsen, K., Hu, S.J. and Carlson, B.E. (2015), "Joining of dissimilar materials", *CIRP Annals - Manufacturing Technology*, available at: <https://doi.org/10.1016/j.cirp.2015.05.006>.
- Munrolive (2020), "Model Y E18: Instrument Panel (IP) Assembly & Comparison MY-M3", Available at: <https://www.youtube.com/watch?v=tPtbgclHkLY> (Accessed: 11 May 2020).
- Redwood, B., Schoeffler, F., Garret, B. (2017), "The 3D Printing Handbook: Technologies, Design and Applications", 3D Hubs B.V.

Zhang, Y., Xu, X. and Liu, Y. (2011), "Numerical control machining simulation: A comprehensive survey", *International Journal of Computer Integrated Manufacturing*, available at:<https://doi.org/10.1080/0951192X.2011.566283>.

Zhu, Z., Dhokia, V.G., Nassehi, A. and Newman, S.T. (2013), "A review of hybrid manufacturing processes - State of the art and future perspectives", *International Journal of Computer Integrated Manufacturing*, available at:<https://doi.org/10.1080/0951192X.2012.749530>.

CHAPTER 2. LITERATURE REVIEW

2.1 Additive Manufacturing on a Large Scale

While Stereolithography was the first 3D printing technology to emerge in 1984 (Hull *et al.*, 1984), the AM process of Fused Filament Fabrication (FFF) disclosed in a 1989 patent by the Minneapolis Minnesota based company Stratasys has become the most widespread (Crump, 1989). These systems take a digital file from computer-aided design (CAD) software and use computer-aided manufacturing (CAM) algorithms to slice the 3D object into 2.5D layers that the system will build one at a time to

approximate the desired CAD geometry (Gibson *et al.*, 2015).

This layer-based approach creates a tradeoff between the level of accuracy in re-creating geometry

using very thin layers and

achieving faster processing times by using thick layers (McMains, 2005). Early efforts focused on minimizing the error through thin layers or finding a balance between build time and stair-step error.

More recently, Oak Ridge National Laboratory and Lockheed Martin presented Big Area Additive Manufacturing (BAAM), which uses thick layers, on the scale of multiple

millimeters, to print large objects up to 100x faster than typical FFF systems (Holshouser *et al.*,

2013). While traditional FFF uses a drive motor to force a polymer filament into a liquefier to generate the pressure needed to extrude material (Figure 2.2a), BAAM uses a screw extruder

similar to those used on polymer processing lines (Figure 2.2b) (Chesser *et al.*, 2019; Turner *et*

al., 2014). Not only does this configuration allow BAAM to process material at a higher rate, but

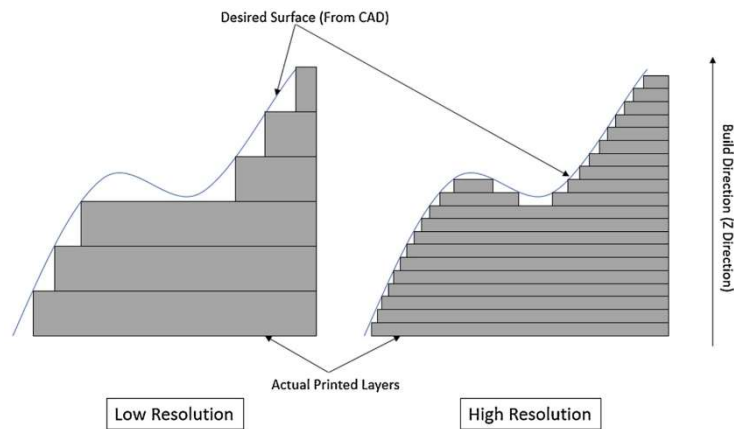


Figure 2.1 The effect layer thickness has on the ability to reproduce a surface geometry (Chesser *et al.*, 2019).

it also allows for the use of low-cost pellet feedstock, which is the standard in the polymer processing industry. Other companies have also demonstrated large scale AM systems based on screw extruders, including Thermwood's LSAM (Thermwood Corporation, 2019), Stratasys' Infinite Build 3D Demonstrator (Librett, 2016), Hybrid Technologies' AMBIT PE-1 (Northrup, 2019), and Filabot's Massive Dimension Direct Pellet Head Extruder (Filabot, 2018).

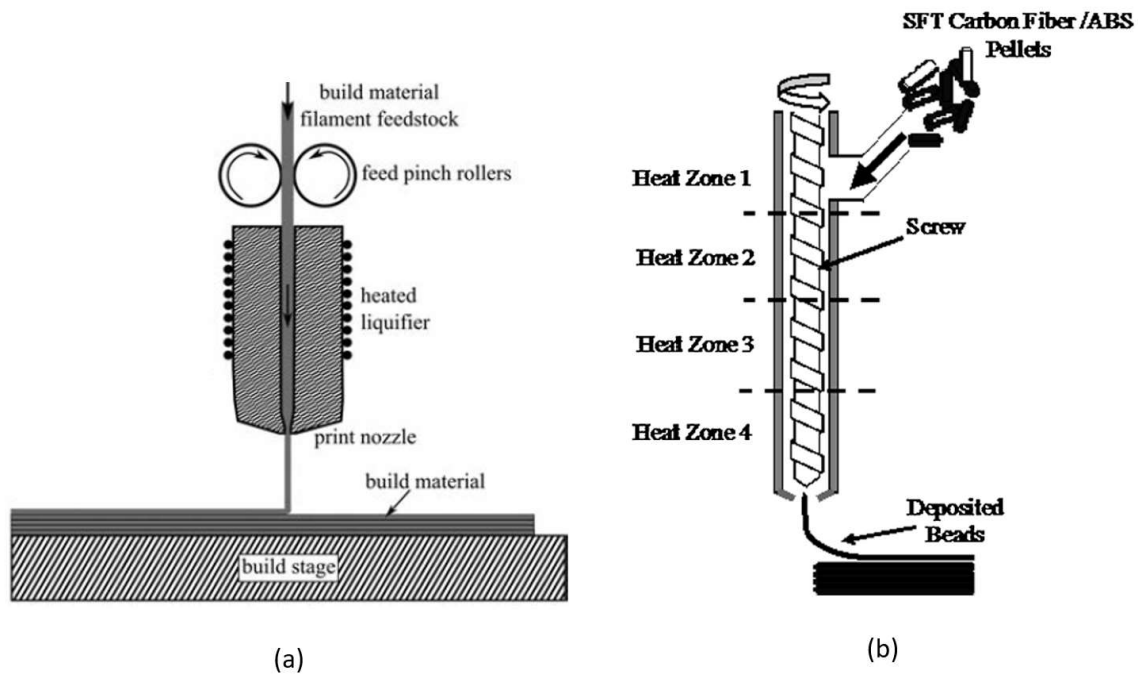


Figure 2.2 A comparison between (a) FFF and (b) BAAM, which uses a screw extruder (Chesser *et al.*, 2019; Turner *et al.*, 2014).

Research, development, and innovation in the area of large scale AM has not been without challenges. Challenges controlling the flow rate, leading to irregular surface geometry and large amounts of porosity led to the integration of a tamping system in BAAM (Duty *et al.*, 2017a). Controlling the extrusion rate has also proven more challenging with the screw extruder than with directly driven filament, which allows for precise metering (Chesser *et al.*, 2019).

There have also been several studies into improving interlayer bond strength, which is more difficult in BAAM due to the lack of a controlled chamber temperature (Kishore *et al.*, 2017). Sun *et al.* demonstrated that the processing conditions inside an FFF build chamber have a strong effect on the bond strength in parts (Sun *et al.*, 2008). This finding demonstrates that it is essential to tailor thermal process parameters to fit each AM system if the structural properties of the parts are essential. Northrup conducted the only published evaluation of the AMBIT PE-1 screw extrusion system but has not reported any thermal characteristics of the system and how they relate to the strength of the resulting part (Northrup, 2019).

2.2 Hybrid Additive and Subtractive Manufacturing

The stair-step error in metal AM did not provide a surface finish or dimensional accuracy that could meet requirements of precision components, which led to the development of the hybrid process Shape Deposition Modeling (SDM) which alternates between adding thick layers and 5-axis contour and planar machining

(Merz *et al.*, 1994). SDM could also be used to create components consisting of multiple materials as long as the melting temperatures were close enough to ensure re-melt and fusion with the previous layer, and coefficients of thermal expansion were close enough to not cause excessive residual stress upon cooling (Fessler *et al.*, 1996; Weiss *et al.*, 1997). Another HM process is the pairing of Directed Energy Deposition (DED) additive processes with CNC machining centers to develop in-envelope hybrid systems using laser

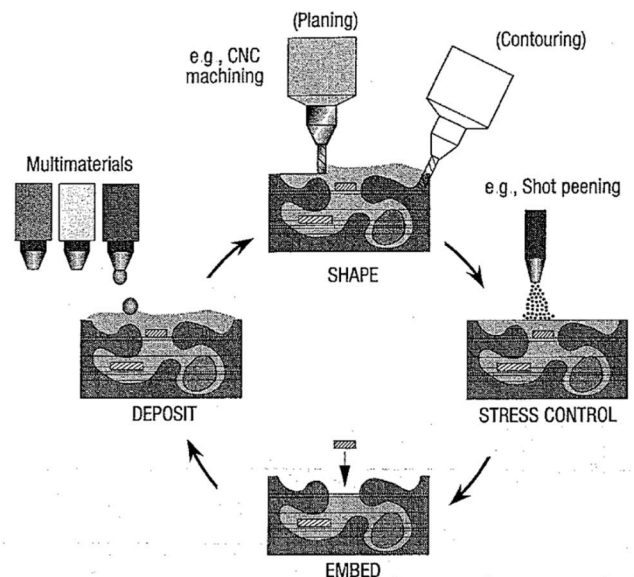


Figure 2.3 Shape Deposition Manufacturing of heterogeneous objects (Weiss *et al.*, 1997)

processes with CNC machining centers to develop in-envelope hybrid systems using laser

cladding (Jeng and Lin, 2001) and gas metal arc welding (Song *et al.*, 1998). Hur *et al.* demonstrate the ability for in-envelope hybrid systems to overcome the challenges CNC machining has with undercut geometry, by selectively slicing layers to maintain visibility (Figure 2.4) (Hur *et al.*, 2002). A different approach is Out-of-envelope hybrid systems that can link together multiple processes in serial to achieve some of the same synergies as in-envelope hybrid systems even though they may require more human intervention. An example of such a system is the pairing of powder bed fusion AM and subtractive machining through the integration of fixturing into the process plan (Frank *et al.*, 2017).

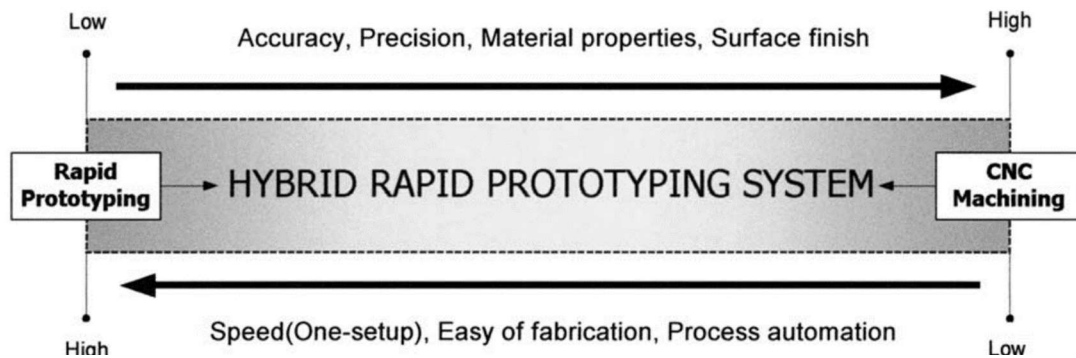


Figure 2.4 Comparison between characteristics of CNC machining and AM (Hur *et al.*, 2002).

Similar synergies exist for these systems when producing parts in materials other than metals. The large scale polymer AM system can use machining to achieve the surface finish and dimensional accuracies required by the system design while maintaining the high levels of productivity achieved through large extrusion volumes (Love, 2015). There has also been significant research in the area of hybrid manufacturing of multiple material components consisting of metal-metal, metal-ceramic, and even polymer-polymer systems (Bandyopadhyay and Heer, 2018). However, research into hybrid manufacturing of polymer-metal systems has been mostly confined to non-structural electronics applications (MacDonald and Wicker, 2016).

There is potential for similar benefits to be achieved in polymer-metal multiple material hybrid manufacturing as have been achieved in dissimilar metals or metal-ceramics.

2.3 Multiple Material Components

Material selection is an essential step in the design process, where functional requirements are aligned with material properties (Ashby and Johnson, 2014). There are many frameworks to guide the material selection process, which must account for many factors, including mechanical properties, chemical properties, manufacturing properties, electrical properties, cost, aesthetics, and more (Rao and Davim, 2008).

When the properties of a single material cannot adequately meet the requirements for a component, multiple materials can be used to create regions with locally tailored properties. An example of this is multi-material injection



Figure 2.5 Rigid polymer component with an overmolded flexible gasket (Protolabs, 2018).

molded components that may have a rigid structure with a more pliable secondary

material overmolded, with each region meeting different functional requirements of the part (Figure 2.5) (Islam *et al.*, 2010). Having unique properties allows the designer to take advantage of complimentary properties and achieve synergies like those found in hybrid manufacturing processes. An example of this is polymer-metal hybrid components used in the automotive industry. These parts take advantage of the structural properties of metal and the ability to produce complex, lightweight structures via polymer injection molding (Grujicic *et al.*, 2008).

Due to challenges with material compatibility, these components often rely on mechanically

interlocking features to join the metal and polymer regions of the part. Despite the popularity of multiple material components in injection molding, adhesion remains a challenge here as well, and mechanical interlocks are often recommended as a backup or replacement for surface adhesion even in polymer-polymer systems (Figure 2.6) (GLS Corporation, 2004; Protolabs, 2018)

Integrating multiple material regions into a single part has also become popular in AM research. Multiple polymers can be integrated into single components using material jetting (Vidimče *et al.*, 2013) and material extrusion systems (Kang *et al.*, 2016). Functionally graded components consisting of multiple metal regions have been created using directed energy deposition (Carroll *et al.*, 2016) and powder bed fusion AM technologies (Yan *et al.*, 2016). Metal-ceramic functionally graded materials have also been produced using AM (Zhang *et al.*, 2019). However, a review of the literature does not mention metal-polymer components

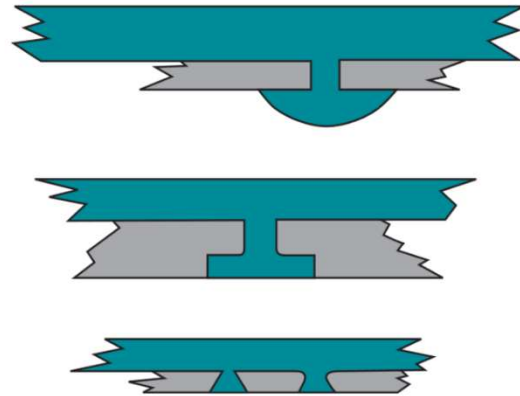


Figure 2.6 Mechanical interlocks used in multi-material injection molded components (GLS Corporation, 2004).

outside of the suspension of metallic powders in a polymer matrix or the incorporation of conductive traces for electronics into polymer components (Bandyopadhyay and Heer, 2018). This gap may be due to the challenge of producing adequate surface adhesion between metals and polymers, challenges producing adequate holding pressures with AM, and the complexity of surface preparation needed (Kauffer, 2011). There is also a lack of a proven mechanical interlock or root structure similar to those that exist for multiple material injection molding.

2.4 References

- Ashby, M.F. and Johnson, K. (2014), "Materials and Design: The Art and Science of Material Selection in Product Design: Third Edition", available at: <https://doi.org/10.1016/C2011-0-05518-7>.
- Bandyopadhyay, A. and Heer, B. (2018), "Additive manufacturing of multi-material structures", *Materials Science and Engineering R: Reports*, available at: <https://doi.org/10.1016/j.mser.2018.04.001>.
- Carroll, B.E., Otis, R.A., Borgonia, J.P., Suh, J.O., Dillon, R.P., Shapiro, A.A., Hofmann, D.C., et al. (2016), "Functionally graded material of 304L stainless steel and inconel 625 fabricated by directed energy deposition: Characterization and thermodynamic modeling", *Acta Materialia*, available at: <https://doi.org/10.1016/j.actamat.2016.02.019>.
- Chesser, P., Post, B., Roschli, A., Carnal, C., Lind, R., Borish, M. and Love, L. (2019), "Extrusion control for high quality printing on Big Area Additive Manufacturing (BAAM) systems", *Additive Manufacturing*, available at: <https://doi.org/10.1016/j.addma.2019.05.020>.
- Crump, S. (1989), "APPARATUS AND METHOD FOR CREATING THREE-DIMENSIONAL OBJECTS", *United States Patent and Trademark Office*, available at: https://doi.org/10.2116/bunsekikagaku.28.3_195.
- Duty, C.E., Kunc, V., Compton, B., Post, B., Erdman, D., Smith, R., Lind, R., et al. (2017), "Structure and mechanical behavior of Big Area Additive Manufacturing (BAAM) materials", *Rapid Prototyping Journal*, available at: <https://doi.org/10.1108/RPJ-12-2015-0183>.
- Fessler, J., Merz, R., Nickel, A., Prinz, F. and Weiss, L. (1996), "Laser deposition of metals for shape deposition manufacturing", *Solid Freeform Fabrication Symposium Proceedings, University of Texas at Austin*.
- Filabot (2018), "New MDPH2 Pellet Head Extruder for Large Format 3D Printing", Filabot Blog, 30 December. Available at: <https://www.filabot.com/blogs/news/new-mdph2-pellet-head-extruder-for-large-format-3d-printing> (Accessed: 11 May 2020)
- Frank, M.C., Harrysson, O., Wysk, R.A., Chen, N., Srinivasan, H., Hou, G. and Keough, C. (2017), "Direct Additive Subtractive Hybrid Manufacturing (DASH): An Out of Envelope Method", *Solid Freeform Fabrication Symposium*, available at: https://doi.org/10.7449/2017/MST_2017_366_368.
- Gibson, I., Rosen, D. and Stucker, B. (2015), "Additive Manufacturing Technologies: 3D Printing, Rapid Prototyping, and Direct Digital Manufacturing, Second Edition", available at: <https://doi.org/10.1007/978-1-4939-2113-3>.

- GLS Corporation, (2004), "Overmolding Guide", available at:
https://www.polyone.com/sites/default/files/resources/Overmold_Design_Guide.pdf
 (Accessed: 11 May 2020)
- Grujicic, M., Sellappan, V., Omar, M.A., Seyr, N., Obieglo, A., Erdmann, M. and Holzleitner, J. (2008), "An overview of the polymer-to-metal direct-adhesion hybrid technologies for load-bearing automotive components", *Journal of Materials Processing Technology*, available at:<https://doi.org/10.1016/j.jmatprotec.2007.06.058>.
- Holshouser, C., Newell, C., Palas, S., Martin, L., Duty, C., Love, L., Kunc, V., et al. (2013), "Out of bounds additive manufacturing", *Advanced Materials and Processes*, Vol. 171 No. 3, pp. 15–17.
- Hull, C.W., (1984), "Apparatus for production of 3D objects by stereolithography", *United States Patent*.
- Hur, J., Lee, K., Zhu-Hu and Kim, J. (2002), "Hybrid rapid prototyping system using machining and deposition", *CAD Computer Aided Design*, available at:[https://doi.org/10.1016/S0010-4485\(01\)00203-2](https://doi.org/10.1016/S0010-4485(01)00203-2).
- Islam, A., Hansen, H.N. and Bondo, M. (2010), "Experimental investigation of the factors influencing the polymer-polymer bond strength during two-component injection moulding", *International Journal of Advanced Manufacturing Technology*, available at:<https://doi.org/10.1007/s00170-009-2507-8>.
- Jeng, J.Y. and Lin, M.C. (2001), "Mold fabrication and modification using hybrid processes of selective laser cladding and milling", *Journal of Materials Processing Technology*, available at:[https://doi.org/10.1016/S0924-0136\(00\)00850-5](https://doi.org/10.1016/S0924-0136(00)00850-5).
- Kang, H.W., Lee, S.J., Ko, I.K., Kengla, C., Yoo, J.J. and Atala, A. (2016), "A 3D bioprinting system to produce human-scale tissue constructs with structural integrity", *Nature Biotechnology*, Vol. 34 No. 3, pp. 312–319.
- Kauffer, P.H. (2011), "Injection Molding: Process, Design, and Applications, Injection Molding: Process, Design, and Applications"
- Kishore, V., Ajinjeru, C., Nycz, A., Post, B., Lindahl, J., Kunc, V. and Duty, C. (2017), "Infrared preheating to improve interlayer strength of big area additive manufacturing (BAAM) components", *Additive Manufacturing*, available at:<https://doi.org/10.1016/j.addma.2016.11.008>.
- Livrett, C. (2016), "3D Demonstrators Designed for Bigger, Lighter Auto and Aerospace Parts", Stratasys Blog, 24 August. Available at: <http://blog.stratasys.com/2016/08/24/infinite-build-robotic-composite-3d-demonstrator/> (Accessed: 11 May 2020).
- Love, L.J. (2015), "Utility of Big Area Additive Manufacturing (BAAM) For The Rapid Manufacture of Customized Electric Vehicles", *United States*, available at:<https://doi.org/10.2172/1209199>.

- MacDonald, E. and Wicker, R. (2016), "Multiprocess 3D printing for increasing component functionality", *Science*, available at:<https://doi.org/10.1126/science.aaf2093>.
- McMains, S. (2005), "Layered manufacturing technologies", *Communications of the ACM*, available at:<https://doi.org/10.1145/1064830.1064858>.
- Merz, R., Ramaswami, R., Terk, K. and Weiss, M. (1994), "Shape Deposition Manufacturing", *The Solid Freeform Fabrication Symposium*.
- Northrup, J. (2019), "Durability of Hybrid Large Area Additive Tooling for Vacuum Infusion of Composites", M.S. Thesis, Brigham Young University, Provo, available at: <https://scholarsarchive.byu.edu/etd/7759>
- Protolabs, (2018), "Design Essentials for Injection Molding", Protolabs Inc., available at: <https://get.protolabs.com/im-essentials-dg/> (Accessed: 11 May 2020)
- Rao, R. V. and Davim, J.P. (2008), "A decision-making framework model for material selection using a combined multiple attribute decision-making method", *International Journal of Advanced Manufacturing Technology*, available at:<https://doi.org/10.1007/s00170-006-0752-7>.
- Song, Y., Park, S., Hwang, K., Choi, D., Jee, H. (1998) "3D Welding and Milling for Direct Prototyping of Metallic Parts", *The Solid Freeform Fabrication Symposium*.
- Sun, Q., Rizvi, G.M., Bellehumeur, C.T. and Gu, P. (2008), "Effect of processing conditions on the bonding quality of FDM polymer filaments", *Rapid Prototyping Journal*, available at:<https://doi.org/10.1108/13552540810862028>.
- Thermwood Corporation (2019), "Thermwood Introduces the LSAM MT", Available at: <https://youtu.be/yHLD4Bj0Me8> (Accessed: 11 May 2020).
- Turner, B.N., Strong, R. and Gold, S.A. (2014), "A review of melt extrusion additive manufacturing processes: I. Process design and modeling", *Rapid Prototyping Journal*, available at:<https://doi.org/10.1108/RPJ-01-2013-0012>.
- Vidimčec, K., Wang, S.P., Ragan-Kelley, J. and Matusik, W. (2013), "OpenFab: A programmable pipeline for multi-material fabrication", *ACM Transactions on Graphics*, available at:<https://doi.org/10.1145/2461912.2461993>.
- Weiss, L.E., Merz, R., Prinz, F.B., Neplotnik, G., Padmanabhan, P., Schultz, L. and Ramaswami, K. (1997), "Shape Deposition Manufacturing of Heterogeneous Structures", *Journal of Manufacturing Systems*, available at:[https://doi.org/10.1016/S0278-6125\(97\)89095-4](https://doi.org/10.1016/S0278-6125(97)89095-4).
- Yan, W., Ge, W., Smith, J., Lin, S., Kafka, O.L., Lin, F. and Liu, W.K. (2016), "Multi-scale modeling of electron beam melting of functionally graded materials", *Acta Materialia*, available at:<https://doi.org/10.1016/j.actamat.2016.06.022>.

Zhang, C., Chen, F., Huang, Z., Jia, M., Chen, G., Ye, Y., Lin, Y., et al. (2019), “Additive manufacturing of functionally graded materials: A review”, *Materials Science and Engineering A*, available at: <https://doi.org/10.1016/j.msea.2019.138209>.

CHAPTER 3. MECHANICAL ROOT STRUCTURE FOR MULTI-MATERIAL HYBRID ADDITIVE AND SUBTRACTIVE MANUFACTURING

Eric Weflen, Matthew C. Frank

*Industrial and Manufacturing Systems Engineering Department, Iowa State University,
Ames, Iowa 50011, USA*

Modified from a manuscript to be submitted to Rapid Prototyping Journal

3.1 Abstract

This research presents a novel method for producing multi-material components produced through in-envelope hybrid additive and subtractive manufacturing. By hybridizing the material composition in addition to the fabrication process, functional requirements can be met more effectively than through homogenous material parts produced in a single manufacturing process. The work is conducted on a large-scale additive manufacturing system added to a 5-axis HAAS machining center through the integration of an AMBIT PE-1 screw extrusion fabrication tool. In this research, the ability to reduce warping in overhang sections is first investigated by enforcing a minimum layer time. The effect of this minimum layer time on the interlayer strength of the printed material is evaluated. Also, a mechanically interlocking root structure is developed, in order to form a mechanical interface between a machined aluminum region, and a carbon fiber reinforced Acrylonitrile Butadiene Styrene (ABS) region deposited with the additive manufacturing tool. The tensile strength of the root structure is measured and found to be on the same order of magnitude as the bulk 3D printed polymer. By targeting the material properties to the local functional requirements within a part, and by taking advantage of both additive and subtractive manufacturing processes, this work will enable broader design options and optimization of performance metrics.

3.2 Introduction

Hybrid manufacturing (HM) systems merge multiple processes into a system to take advantage of their strengths while avoiding weaknesses (Lauwers *et al.*, 2014). These processes can be single, in-envelope systems, or conducted in a serial out-of-envelope set of steps across multiple machines. In-envelope systems have the advantage of reducing the need for human intervention to re-fixture and find the origin of the part, both reducing the risk of error and simplifying process planning.

Additive manufacturing (AM) has been combined with subtractive processes like machining with much success due to the complimenting strengths of each process (Zhu *et al.*, 2013). AM can produce complex geometries without the need for tooling but needs to balance dimensional accuracy and surface finish with productivity. Machining can be used to improve the surface finish and dimensional accuracy of near net shape AM parts similarly to how it is implemented as a post-processing step in the metal casting industry.

While subtractive processes start from a homogenous stock of material to produce a part, AM and HM can locally align the material properties and composition to match the functional requirements of the part (Liu *et al.*, 2017). Similar to the heterogeneous material structures found in nature, these parts can reduce the tradeoffs made during material selection such as weight, strength, stiffness, or hardness. However, the interfaces between different material regions can be a point of failure, which has led to the development of functionally graded materials, which gradually change the composition from one material to the next. This solution works well for materials with similar processing properties, such as melt temperature, but may not be compatible with materials that are dissimilar such as metals and polymers.

There are a limited number of mechanisms that can be used to bring together different material regions, including mechanical, chemical, thermal (fusion or solid-state), or a hybrid combination of these (Martinsen *et al.*, 2015). Since metals and polymers have such different processing properties, it may be challenging to achieve thermal bonding (Figure 3.1). While it may be possible to achieve a chemical bond, it would require the application of an adhesion promoter, which would require an intervention mid-process (Albert *et al.*, 2015).

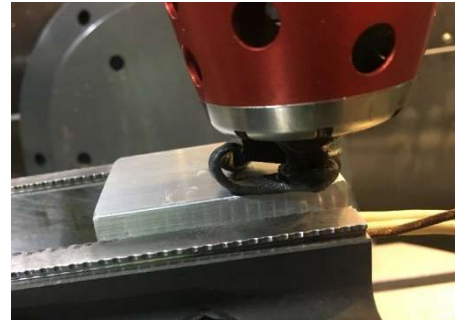


Figure 3.1 Extruded polymer fails to adhere to a clean aluminum surface.

Alternatively, a mechanical bond can be formed through the creation of a surface structure in the metal that allows the polymer to bond upon deposition. This bond can be achieved by creating an undercut in a metal structure, into which the polymer can be extruded and solidified, forming a mechanically interlocking root-like structure similar to those used in industrial applications like the root of a gas turbine blade (Figure 3.2). While a similar system employing undercuts to bond metal and polymer regions together has been implemented in a hybrid hydroforming-injection molding process (Albert *et al.*, 2015, 2019), a system like this does not exist for hybrid additive and subtractive manufacturing.

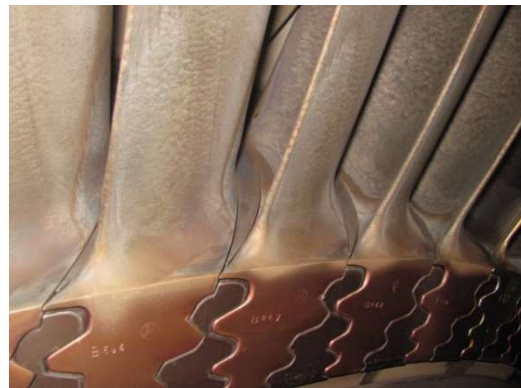


Figure 3.2 Mechanical interlocking features retain gas turbine blades (Combined Cycle Journal, 2012).

This research presents a method for producing metal-polymer components in hybrid additive and subtractive manufacturing systems. We begin by testing material performance and

process parameters of a material extrusion additive manufacturing tool integrated into a machining center. Next, we present a method for forming a mechanical root structure to form a joint between metal and polymer regions that is compatible with a hybrid additive and subtractive system. Finally, we evaluate the strength of the root structure for comparison with the strength of the bulk extruded material.

3.3 Related Work

Additive manufacturing processes must strike a balance between the level of productivity and their ability to accurately reproduce surface geometries and the associated surface roughness (Jones, 2014). Thick layers allow for faster printing but at the cost of increased stair-step error inherent to layer-based manufacturing processes (Chesser *et al.*, 2019). While traditional fused filament fabrication (FFF) systems strike a balance between these tradeoffs, researchers at Oak Ridge National Laboratory demonstrated the ability produce large objects over 100x faster by using a layer thickness on the scale of multiple millimeters (Duty *et al.*, 2017a). Since the traditional FFF extruder, using a small filament forced into a heated nozzle, could not meet the necessary flowrate, they used a screw extruder similar to those used in industrial polymer extrusion systems (Duty *et al.*, 2015).

One approach taken to maintain dimensional accuracy and surface finish while improving productivity through thick layers has been to create a hybrid process merging both additive and subtractive manufacturing in-envelope (Lorenz *et al.*, 2014). HM can avoid the weaknesses of each process while exploiting their strengths to achieve a system with capabilities greater than each process individually (Lauwers *et al.*, 2014; Zhu *et al.*, 2013). The advantages of hybrid additive and subtractive processes have been exploited heavily in the production of metal components, with complex geometry being produced with AM, and areas needing precise

dimension or surface finish being machined (Fessler *et al.*, 1996; Flynn *et al.*, 2016; Jeng and Lin, 2001). HM has also been used for the production of polymer components, as well as components consisting of multiple materials (Love, 2015; MacDonald and Wicker, 2016).

While HM merges multiple processes to create a synergistic effect, the same concept can be applied to material selection of a component by merging multiple materials into a single part (Gupta and Tandon, 2015). In injection molding, it has been common to produce components existing with both rigid and flexible regions through overmolding in order to meet functional requirements more effectively (Islam *et al.*, 2010). Researchers have been able to take advantage of computer algorithms such as topology optimization and artificial intelligence to design complex multi-material parts to meet specifications created by a design engineer (Hiller and Lipson, 2009). Metal-polymer multi-material components have been implemented in the automotive industry, with the hydroformed aluminum regions providing structure and overmolded polymer regions forming lightweight, complex geometries (Grujicic *et al.*, 2008). While AM has also been used to create parts with locally specified material properties, including components consisting of polymer-polymer, metal-metal, and ceramic-metal regions, a review of the literature does not turn up any metal-polymer systems outside of the integration of electronics, or the use of metal fillers in a polymer matrix (Zhang *et al.*, 2019). There is an opportunity to achieve similar benefits by producing metal-polymer components using hybrid additive and subtractive manufacturing. A Challenge of producing parts comprised of dissimilar materials is creating a robust interface (Martinsen *et al.*, 2015). While mechanical fasteners could be used, they are not ideal for an integrated, automated system, leaving an opportunity for a specialized joining method to be developed for dissimilar materials in an HM environment.

3.4 Solution Overview

As mentioned above, this work develops a method to mechanically join dissimilar materials and begins with a study of the requisite parameters for printing the plastic feedstock. First, we investigated and refined process parameters using the laboratory hybrid setup. In that system, additive manufacturing capabilities are added to a CNC machining center through the implementation of an AMBIT PE-1 tool, which uses a screw extruder similar to that used on the Big Area Additive Manufacturing (BAAM) system (Duty *et al.*, 2017b). Process parameters and the resulting strength of the printed polymer are evaluated to act as a baseline for the strength of the inter-material joint. For the root structure, we borrow the undercut geometry of the dovetail joint, which has a long history as a structural joint in woodworking, masonry, and metalworking. A dovetail groove is machined in the aluminum region (Figure 3.3a), and carbon fiber reinforced Acrylonitrile Butadiene Styrene (ABS/CF) is extruded into the groove to create a joint on to which the polymer region is to be deposited (Figure 3.3b). As the ABS/CF solidifies, it becomes solid, locking it in place. Finally, the regions of the part requiring improved surface finish or dimensional accuracy can be machined (Figure 3.3c).

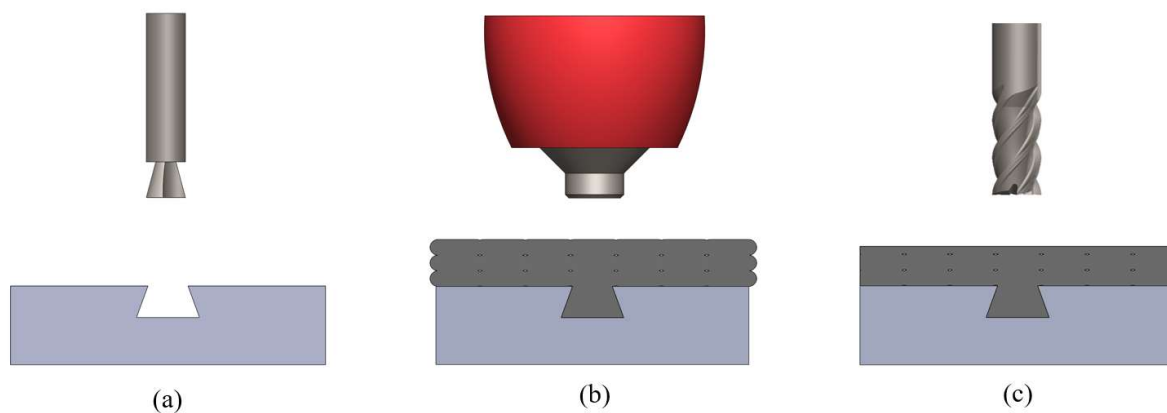


Figure 3.3 The process for creating a mechanical root structure in the material interface. a) A dovetail cutting tool is used to create an undercut feature in an aluminum block. b) The root feature is filled with ABS/CF polymer, and the desired geometry is 3D printed. c) A cutting tool is used to improve surface finish and dimensional accuracy where required.

It is essential to understand that as the polymer solidifies and cools, it will have a significant size reduction due to crystallization, undergoing a phase change, and a greater coefficient of thermal expansion as compared to the metal. Pairing these challenges with the low level of surface adhesion with the aluminum would cause polymer in a simple straight-line groove to retract and loosen in the dovetail profile (Figure 3.4a). However, a closed contour, such as the circle seen in Figure 3.4b, will cause the polymer to shrink-fit in the feature upon solidification.

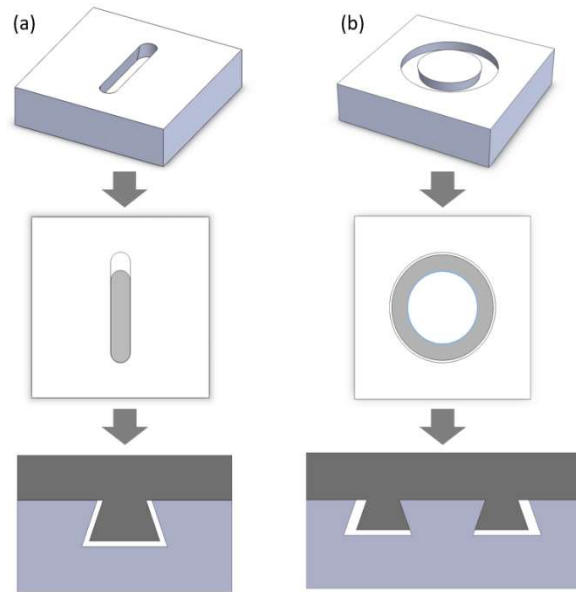


Figure 3.4 a) Open-ended versus b) closed-loop contour for dovetail feature.

By using this technique within a 5-axis machining center, complex metallic geometries can be created, then paired with complex polymer geometries. Figure 3.5a shows an example of

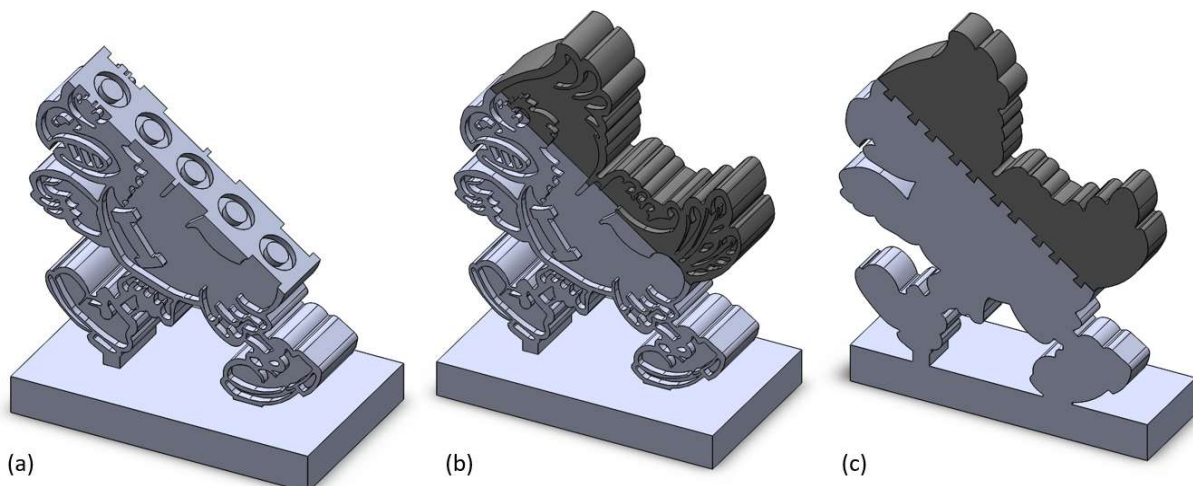


Figure 3.5 Metal-polymer multi-material component. a) Machined aluminum region with root features in the interface. b) Aluminum and ABS/CF multi-material component. c) Cross-section exposing the material interface.

an aluminum component with five circular mechanical interlocking features along the interface. Following the process described above, a metal-polymer object can be created using a mechanical bond via the dovetail features seen in the cross-section view in Figure 3.5c. The process parameters and, in particular, the cooling of the plastic after deposition is critical to this process. The following section presents a study of the cooling effects by enforcing a minimum layer time on the properties of the resulting part.

3.5 Effect of Process Parameters and Cooling

The influence of cooling time on the geometric stability of the printed parts was evaluated by printing an overhang test part (Figure 3.6). Since the polymer extrusion tool used does not have active cooling, we implemented a pause at the end of each layer to allow the part to cool. Our control condition was no pause on the overhang test geometry, which results in a 30 second layer time. A pause was added to achieve different layer times, and all other parameters were held constant. ABS with a 20% fill of chopped carbon fibers (ABS/CF)

(Hybrid Manufacturing Technologies, McKinney, Texas, USA) was printed using a

UMC750 mill (Haas Automation Inc., Oxnard, California, USA) fitted with the AMBIT PE-1 tool (Hybrid Manufacturing Technologies). Numerical control code was generated using the ORNL Slicer developed by Oak Ridge National Laboratory, using the process parameters listed in table 1. With these parameters, the part consists of 25 layers with a total print time of 12

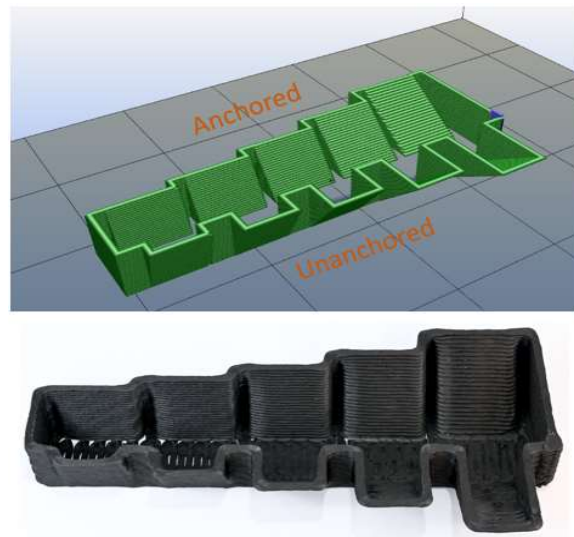


Figure 3.6 Simulated tool paths from the ORNL slicer and the resulting part.

minutes and 28 seconds, making the average layer time approximately 30 seconds. Minimum layer times are established by placing a pause of 0, 30, 90, and 160 seconds at the end of each layer to bring the total layer time to 30, 60, 120, and 180 seconds. The test geometry evaluates two overhang scenarios. The first geometry has walls on either end of the overhang region to better anchor the part to the build platform. The second, and more challenging, is an overhang with unanchored sidewalls (Figure 3.6). A qualitative visual comparison of these parts was conducted.

Table 3.1 Process parameters used in the ORNL Slicer for use with the AMBIT PE-1 tool in a HAAS UMC750 mill.

Parameter	Setting
Temperature	230° C
Nozzle Diameter	5 mm
Layer Thickness	2 mm
Bead Width	6 mm
Feed Rate	46 mm/s
Spindle Speed	110 rpm
Pump On Delay	0.4 s
Pre-Start Spindle Speed	100 rpm
Tip Wipe Distance	12.7 mm
Tip Wipe Speed	56 mm/s

The control sample, printed with no pause for cooling, resulting in a 30-second layer-time and exhibited sagging and warping (Figure 3.7). It was observed during printing that the material did not have sufficient time to solidify, remaining pliable even after several subsequent layers had been printed. This prevented the part from gaining adequate structural integrity to maintain its shape. This sample was the only one to show clear deformation on the anchored overhangs, with upward bow starting at the 25° overhang (Figure 3.7c). This deformation progressively worsened as the angle was increased, with collapsed occurring on the anchored 55° overhang

(Figure 3.7a). On the unanchored overhang, a more challenging test, the 30-second sample showed upward bow starting at the 15° overhang that worsened until the 45° overhang, which saw deformation higher than several layer thicknesses (Figure 3.8). Interestingly, the 55° overhang was an improvement, which may be attributed to gravitational forces counteracting the upward warping.

Samples with 60, 120, and 180 second layer times performed similarly to each other. They reproduced the anchored overhang

geometry with minimal defects and showed less than a single layer thickness of deformation on the unanchored overhang (Figure 3.8). This test demonstrates that having a layer time longer than 30 seconds can help improve geometry reproduction, but we do not see a noticeable benefit of more than 60 seconds. The start and stop location of the layer, often referred to as the z-seam, was less visible when printed with a 60 second layer time (Figure 3.7b). The z-seam is an area prone to defects in large scale additive manufacturing systems, with a less visible seam being more desirable (Chesser *et al.*, 2019; Hassen *et al.*, 2016). It should also be noted that this is a single-walled part with more air exposure and lower thermal mass than a solid part. If the geometry of the part or cooling dynamics of the environment were to change, it would likely affect these results (Sun *et al.*, 2008).

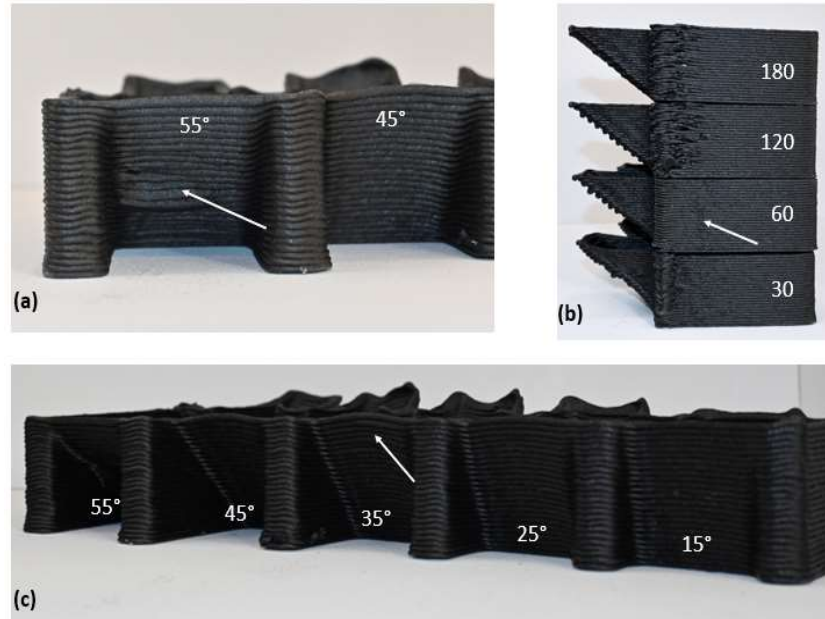


Figure 3.7 Results of 30 second layer time overhang test. a) 55° overhang collapse b) z-seam defects c) supported overhang comparison



Figure 3.8 Un-anchored overhang test samples with 30, 60, 120, 180 second minimum layer time enforced by pausing at the end of each layer.

Since the cooling parameters were expected to impact the bonding between layers of the printed material, we investigated that next. The strength of interlayer bonding along the z-axis of the part was tested following ASTM D638-14. Samples with type III geometry and a thickness of 14mm, as specified in the standard, were cut vertically from a printed piece of ABS/CF with a length, width, and height of 209, 25.4, and 276 mm respectively (Figure 3.9). Minimum layer

time and spindle speed were varied according to Table 3.2 by pausing at the end of each layer in a similar fashion to the overhang test piece. The same printing parameters in Table 3.1 were used for these samples. A waterjet cutter was used to cut four test samples from each printed part, which were then face milled to achieve the final geometry (Figure 3.9). The samples were allowed to equilibrate in the lab environment of 35% humidity and 25° C for at least 24 hours before testing. The cross-section of the tensile sample neck was assessed by

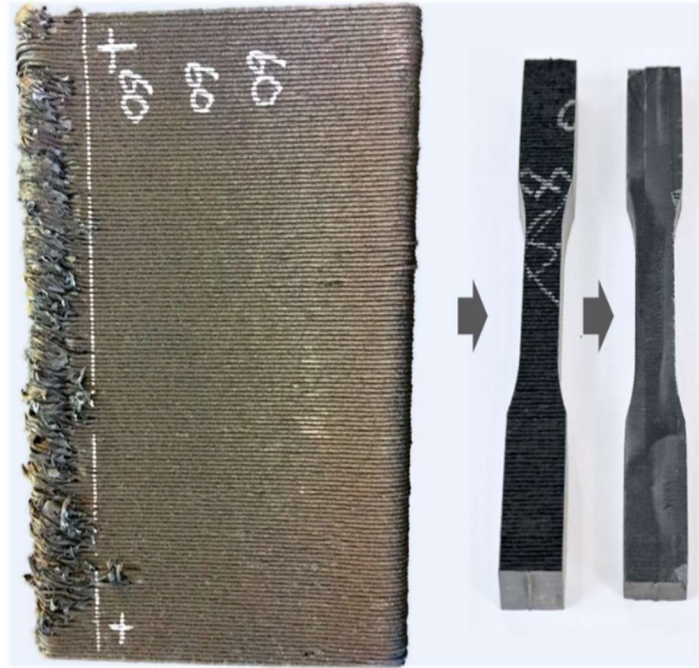


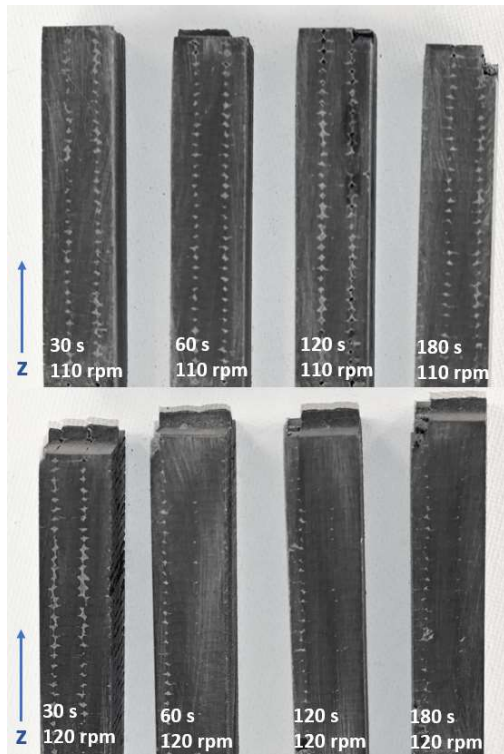
Figure 3.9 Four tensile bars are waterjet cut from each 3D printed slab then machined.

measuring the width and thickness in three locations using a caliper (Mitutoyo, Japan). A UH-F300kNX universal testing machine (Shimadzu Corp., Japan) was used to test the samples, using a strain rate of 5 mm/min.

Table 3.2 The Process parameters used for tensile test samples. Samples that failed outside of the neck region or were damaged during preparation are excluded.

Spindle Speed (rpm)	Layer Time (s)	Samples Tested
110	30	3
110	60	2
110	120	4
110	180	4
120	30	4
120	60	4
120	120	4
120	180	3

It was noted that samples produced with a spindle speed, which influences the material flow rate, set to 110 rpm had visible porosity between deposited beads (Figure 3.10). In the



instance of the 60 second, 110 rpm layer time samples, the inter-bead bonding along the y-axis was so weak that two of the samples broke during machining. While these voids are a known feature of parts produced using FFF, minimizing the void size is a common step during process parameter development (Duty *et al.*, 2017a; Turner and Gold, 2015). This led us to test a second spindle speed, 120 rpm, to see how changing the material flow rate influences the porosity and strength of the part. The samples produced at a spindle speed of

Figure 3.10 Porosity found in samples. 120 rpm exhibited signs of over extrusion (Figure 3.11), where excess material is squeezing upward between deposited beads of ABS/CF. Figure 3.10 shows that using the 120 rpm spindle speed generally reduces the size and quantity of voids.

A balance must be struck between material squeeze-out and the quantity and size of voids in a part. Some commercial systems using nozzles in this size range implement a tamper (Duty *et al.*, 2017a) or a roller (Thermwood Corporation, 2019) to press down the material, reducing voids and eliminating squeeze-out in the z-direction.

These features may make the system less

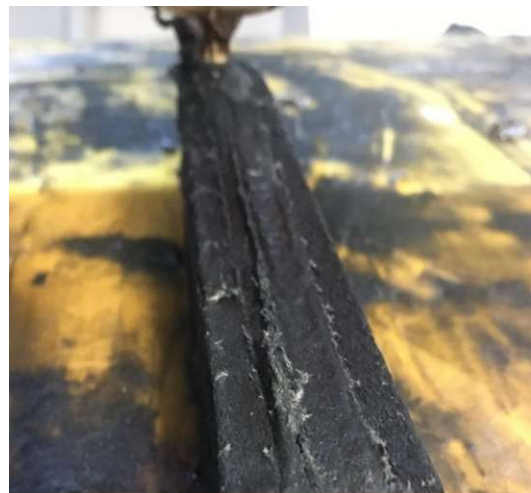


Figure 3.11 Tensile bar slab produced with a spindle speed of 120 rpm has material squeezing upward, a sign of over extrusion.

sensitive to the speed of the screw in the extruder while still producing solid and dimensionally accurate parts (Duty *et al.*, 2017a). Furthermore, Figure 3.10 shows that layer time does not have an apparent impact on the appearance of voids. The exception to this was the 30 second, 120 rpm sample, which shows more porosity than the other samples produced with a 120 rpm spindle speed. This increase in porosity may be due to slumping of the part due to inadequate cooling time for solidification (Figure 3.12). This slumping could increase the gap between the top of the part and the nozzle for successive layers, which may lead to an increase in voids.

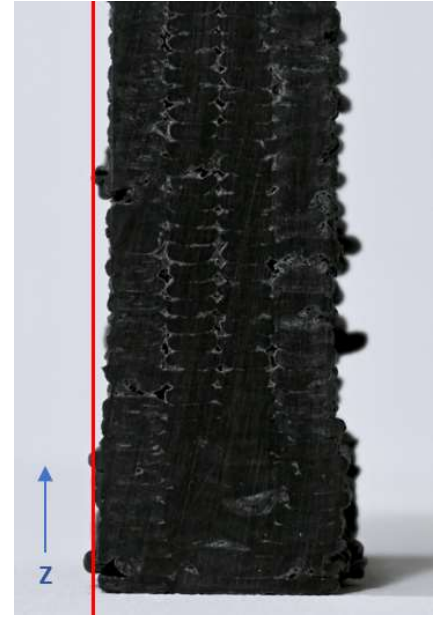


Figure 3.12 Slumping seen in section of printed part with 30s layer times.

Next, the samples were evaluated for tensile strength. The fracture for all test samples occurred at the bonding area between layers (Figure 3.13). It was expected that as the layer time decreased, the interlayer strength would increase. However, it is observed that moving from a 30



Figure 3.13 Fracture surface of a tensile test bar.

second to a 60 second layer time improves the strength of the parts (Figure 3.14). Kishore shows that increasing the surface temperature of the previous layer generally increases inter-layer strength. However, there are diminishing returns after the glass transition temperature of the material is reached (Kishore *et al.*, 2017). Duty demonstrates that by reducing the porosity through tamping an increase in strength is achieved (Duty *et al.*, 2017a). Slumping was noted in the samples produced

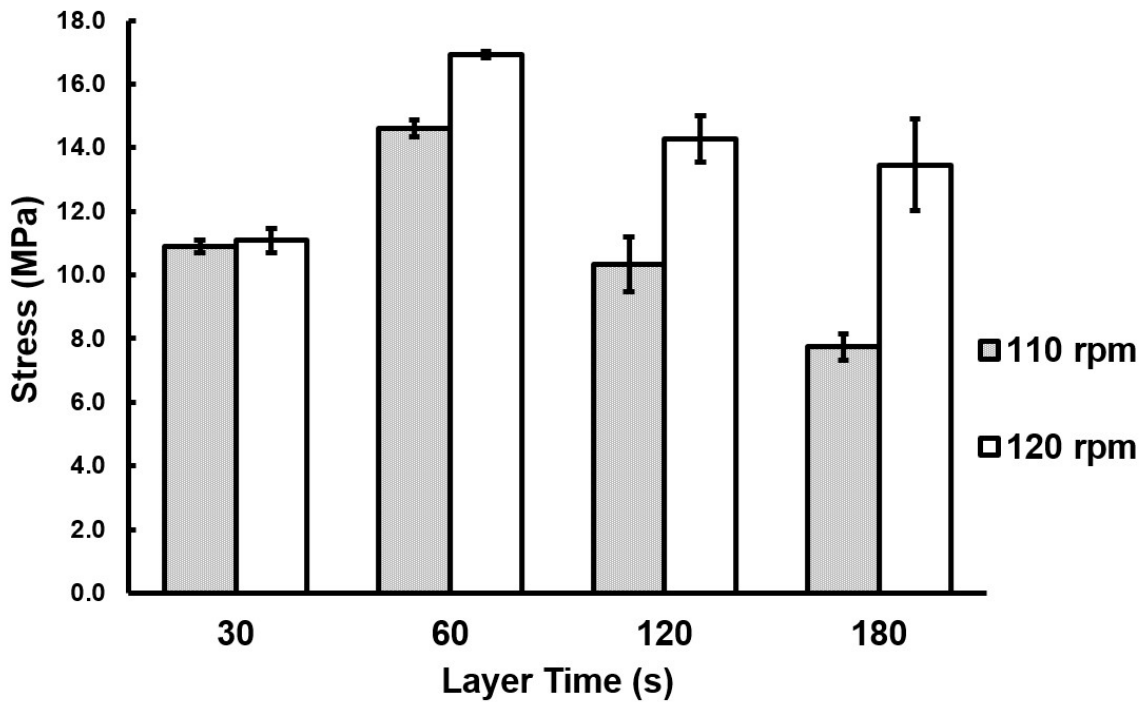


Figure 3.14 Interlayer strength of deposited carbon fiber reinforced ABS along the z-axis of the part. Error bars represent standard error of the mean using four test samples, except for the 110 rpm, 30 second layer time and 120 rpm, 180 second layer time sample sets which only contain three samples and the 110 rpm, 60 second layer time sample set that only contains two samples.

with a 30 second layer time, and Figure 3.10 shows an apparent decrease in porosity when moving from a 30 second layer time to a 60 second layer time for the 120 rpm sample. Possibly, the strength was reduced more by porosity than was gained from reduced cooling time. When the layer time is increased beyond 60 seconds, there is a downward trend in strength. Other researchers have observed a similar trend of inter-layer strength decreasing as the part cools below the ABS glass transition temperature of approximately 100°C (Ajingeru *et al.*, 2018; Kishore *et al.*, 2017). This trend may be due to increased temperatures leading to reduced viscosity of the material, which may increase the formation and inter-molecular diffusion between beads (Sun *et al.*, 2008). A second mechanism leading to this trend may be due to the

longer overall print time of the parts produced with longer layer times. Regions of the part may have remained above the glass transition temperature for more extended periods of time, allowing for a greater diffusion at the interface, which is referred to as the healing phenomenon (Sun *et al.*, 2008).

At this point, we understand the effect of cooling time and spindle speed on the strength of the bulk 3D printed ABS/CF material when processed with the AMBIT PE-1 tool in our machining center. This gives us confidence that a mechanical performance study of a metal-polymer material transition can be performed, owing to the fact that we have an understanding of the bulk material properties of both the aluminum and ABS/CF materials.

3.6 The development of a Mechanical Dovetail Joint

In this section, we evaluate the structural performance of the mechanically interlocking root structures. There are multiple methods by which features can be laid out within the interface between material regions, two of which are evaluated here. The first is a circular feature, which can be duplicated, and nested in the interface cross-section (Figure 3.15 a & b). The second method is to follow the perimeter of the interface, with extra strength being added by concentric nesting. Long, straight geometries may lead to a loss of the shrink fitting seen by the smaller features. This challenge

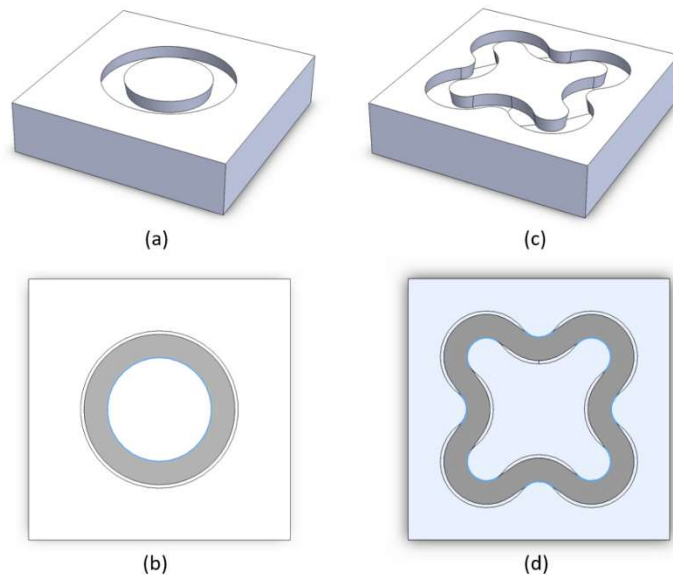


Figure 3.15 A-B) Circular toolpath for the dovetail profile. C-D) A concave-convex toolpath for the dovetail profile.

is overcome by using an alternating concave-convex contour following the perimeter, which maintains a mechanical interference fit at the inside radius of the curve (Figure 3.15 c & d).

To test the strength of these features, we borrowed the sample geometry from ASTM D897-08. A dovetail groove was machined into a 6061 alloy aluminum block, either following either the circular or concave-convex contour (Figure 3.16a). Samples were removed from the mill for drying and preheating to 75°C in a dehydrator (National Presto Industries, Eau Clair, Wisconsin, USA) while a custom-designed heating block was used to preheat the vice to 100°C for a minimum of 3 hours. The machined sample was placed in the vice with the bottom surface in contact with the heating block and allowed to equilibrate for 30 seconds. The extruded ABS/CF did not have sufficient adhesion to the bare aluminum, pulling away from the part before the material can cool (Figure 3.1). Since the root structure does not encompass the entire cross-section of the material transition, we need to have adequate temporary adhesion to retain the molten material and resist warping as it solidifies. A temporary bonding surface was created by solvent casting a film of ABS on the aluminum by applying a coating of an ABS/Acetone solution. This temporary bond was just strong enough to hold the polymer in place during solidification to reduce warping. Once the ABS/CF was solid, the mechanical interlocking of the dovetail root forms the structural joint.

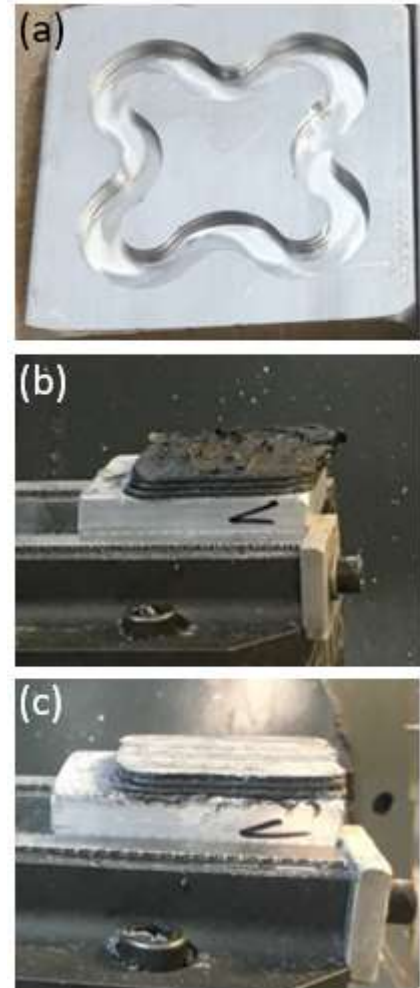


Figure 3.16 Tensile sample is produced by a) machining the dovetail profile in aluminum b) extruding ABS/CF c) machining the printed material.

In order to form a mechanically interlocking root feature, the dovetail channel must be filled entirely with ABS/CF polymer using the AMBIT PE-1 tool. Cross-sections were cut from samples to aid in parameter development to achieve a filled dovetail. A low feed rate of 5.7 mm/s was selected, and the spindle speed was adjusted until there were no voids present in the cross-section (Figure 3.17). In order to achieve a filled channel, a spindle speed of 22 rpm or greater was required. However, this spindle speed led to enough excess material squeezing out of the channel that it could interfere with the AMBIT PE-1 tool as it prints the following layer. This issue was exacerbated by the rapid cooling of the

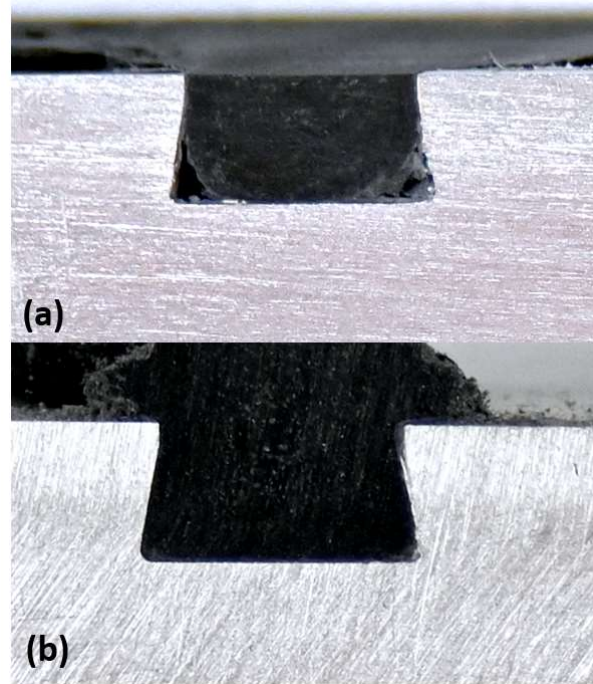


Figure 3.17 a) Dovetail profile is underfilled with polymer b) Dovetail profile with complete fill.

polymer in contact with room temperature aluminum. We overcame this challenge by preheating the aluminum sample and the vise, as mentioned earlier. The preheating allowed the excess polymer to cool slower, remaining pliable long enough for the following layer to be printed without risking damage to the AMBIT PE-1 tool. This heating may also help improve the bond between the root feature and the first printed layer by maintaining a temperature near the glass transition temperature of the ABS/CF (Kishore *et al.*, 2017).

Three layers, totaling six millimeters in height, of ABS/CF, were printed on the 51 mm square cross-section of the part (Figure 3.16b) using the same process parameters listed in Table 3.1. A minimum layer time of 60 seconds was used since that value delivered the strongest

interlaminar bonding. Once the sample was sufficiently cooled, a flat endmill was used to cut the polymer block down to 5mm height to provide a flat surface for adhesive application (Figure 3.16c). West system 650-8 G/flex epoxy (Gougeon Brothers, Inc., Michigan, USA) was used to adhere the top aluminum block to the machined ABS surface. Both surfaces were prepared by sanded with 80-grit sandpaper and washed with 70% isopropyl alcohol according to the manufacturer's recommendation. The samples were allowed to equilibrate in the lab environment of 35% humidity and 25°C for at least 24h before testing. A threaded hole in each aluminum block was used to retain a custom tensile test



Figure 3.18 Tensile test setup for the mechanical interlocking root.

fixture seen in Figure 3.18. Eight samples each of the circular and concave-convex geometry were tested in the Shimadzu universal testing machine at a strain rate of 0.1 in/min

Under tensile loading, the concave-convex perimeter failed at a higher mean force than the circular sample, at 6.5 kN and 3.9 kN, respectively. However, the concave-convex root structure had a greater cross-section at 7.0 cm² compared to 4.2 cm² for the circular root structure. When the force is normalized based on the narrowest root cross-section at the top of the dovetail, there is not a significant difference in force per area using students t-test ($p=0.967$), as seen in Figure 3.19. This demonstrates that the cross-sectional area of the root structures nested in the material transition surface is what will determine the strength of the joint.

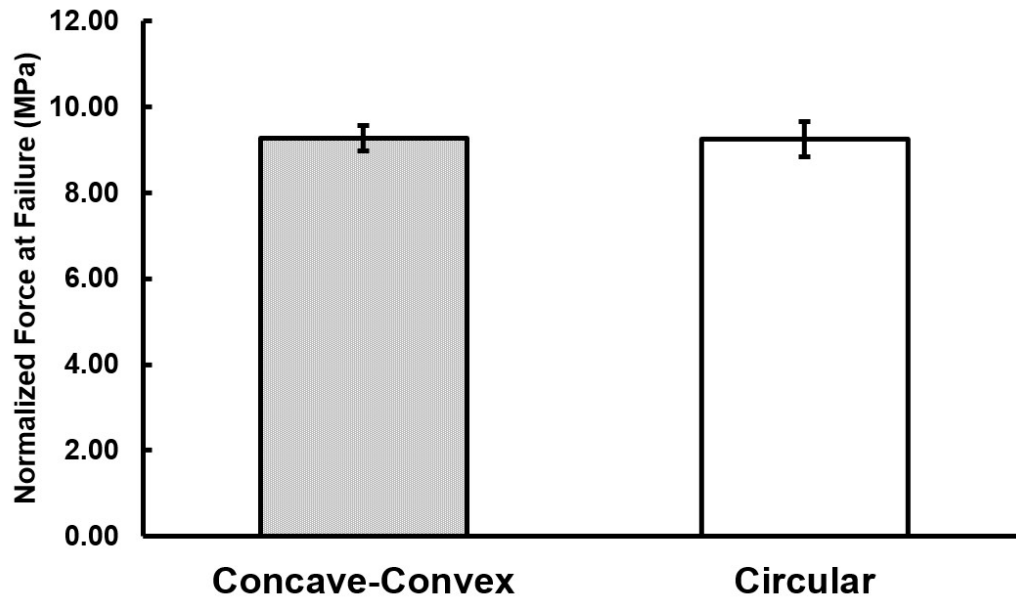


Figure 3.19 Tensile strength of the joint between machined aluminum and extruded ABS/CF normalized by the cross-section of the machined dovetail feature.

The mean stress values at failure for these features are less than all the 3D printed tensile bars except those produced with a 180 second layer time and 110 rpm spindle speed. To

understand why these parts failed at a lower stress value, we evaluate the failure zones of the parts. The test samples typically failed at the top surface of the dovetail feature (Figure 3.20).

This failure mode suggests that the break was due to an adhesive failure between the root structure and the first layer, similar to the interlayer, adhesive failure seen in the previous section cooling time investigation. There were no instances of the dovetail root structure being

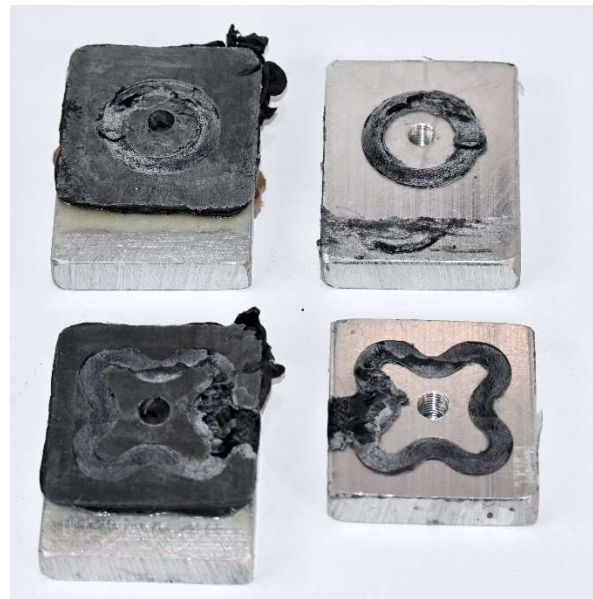


Figure 3.20 Typical tensile test failure for circular and concave-convex root structures.

pulled out of the channel. However, the dovetail feature had started to pull upward out of the channel a small amount and was loose in the channel after the tensile testing was completed. It is possible that this movement of the root contributed to or initiated the failure at the interface and may explain the lower failure point. The lower strength could be caused by the sharp transition at the dovetail top, concentrating stress at the knit line. The material deposited into the dovetail feature also has drastically different cooling dynamics when compared to the tensile bars, which influences the strength of the knit lines. There was a single example for both the circular and the concave-convex features where the failure was through the bulk 3D printed ABS/CF material (Figure 3.21). These samples suggest that the interface bond strength is close to that of the bulk 3D printed ABS/CF in these samples.



Figure 3.21 Bulk 3D printed ABS/CF failure of tensile test samples.

Other loading conditions exist that have not been tested here. If these samples were loaded under shear, we would expect them to fail along the layer line where the 3D printed block of material bonds to the mechanical root, but likely at a lower force due to stress concentration from the sharp edge at the top of the dovetail. Under compressive loading, the root structure is not taking the bulk of the load, and the part should perform similarly to a 3D printed part. In some applications, the root structure may be holding a cantilever component that is being loaded perpendicular to the root, which would put certain regions in compression and others in tension.

This situation would leave a small fraction of the root structure carrying the bulk of the tensile load. Even though our testing did not show the root structure to be the failure initiation point, further evaluation should be conducted for components designed with this loading state in mind.

A designer or algorithm can use these results to plan for or even to tune the strength of the joint to meet the design specifications by changing the packing density of circular features, or by adjusting the spacing between concentric concave-convex profiles. Reduced strength requirements can save machining and printing time by removing such features. It may be desired to have the polymer section to break away at a specific loading, which can be adjusted by changing these features. This could be helpful in cases where break-away is desirable, such as in the automotive components that may sacrificially fail to avoid more costly damage. These break-away features may also be useful in a safety situation to prevent injury.

3.7 Conclusions

This research presented a novel hybrid additive and subtractive approach to manufacture components consisting of dissimilar materials. Aluminum and carbon fiber reinforced ABS were mechanically joined using a dovetail shaped interlocking feature. The effect of cooling time on the geometric accuracy of large-scale printed parts was investigated, showing that adequate cooling time can have an impact of the warping of the part, but with diminishing returns. The consequence this cooling time had on the strength of printed parts was investigated, and it was discovered that some degree of cooling could be beneficial, but beyond 60 seconds of cooling time, the strength drops off. These strengths were compared to the strength of the mechanical root structure, and it is found that for most processing conditions, these components experienced adhesive failure at a lower stress than the bulk 3D printed material. Designers can tune the

strength of the joint between materials by controlling the packing density of mechanical root features, which may be difficult using conventional adhesives.

While aluminum was chosen due to favorable machining characteristics, this approach may be transferable to other metals, such as steel or titanium. Similarly, carbon fiber reinforced ABS polymer was used in this study despite the potential incompatibility with aluminum, due to the abundance of research connected on this material in large scale AM. However, this approach may be compatible with many polymers exhibiting similar shrink rates upon solidification as the material used in this study. This research focused on a single root profile geometry, the dovetail, but there are other methods of creating an undercut feature using subtractive manufacturing. There are also numerous loading conditions that such a joint could experience, which have not been tested here, such as shear, compressive, peel, and cantilever loading of the part. A better understanding of these factors can improve a designer's ability to incorporate these features into a component.

3.8 References

- Ajinjeru, C., Kishore, V., Lindahl, J., Sudbury, Z., Hassen, A.A., Post, B., Love, L., et al. (2018), "The influence of dynamic rheological properties on carbon fiber-reinforced polyetherimide for large-scale extrusion-based additive manufacturing", *International Journal of Advanced Manufacturing Technology*, available at:<https://doi.org/10.1007/s00170-018-2510-z>.
- Albert, A., Drossel, W.G., Zorn, W., Nendel, W. and Raithel, D. (2015), "Process combination of hydroforming and injection moulding for the insitu manufacturing of metal and plastic composite structures", *Materials Science Forum*, available at:<https://doi.org/10.4028/www.scientific.net/MSF.825-826.522>.
- Albert, A., Werner, M., Landgrebe, D., Drossel, W.-G., Layer, M., Engelmann, U. and Kroll, L. (2019), "Media Based Forming and Injection Molding Based on Fiber Reinforced Plastic Tubes", *Procedia Manufacturing*, available at:<https://doi.org/10.1016/j.promfg.2018.12.060>.
- ASTM-D638-14. (2014), "Standard Test Method for Tensile Properties of Plastics", *ASTM Standards*.

- Chesser, P., Post, B., Roschli, A., Carnal, C., Lind, R., Borish, M. and Love, L. (2019), “Extrusion control for high quality printing on Big Area Additive Manufacturing (BAAM) systems”, *Additive Manufacturing*, available at: <https://doi.org/10.1016/j.addma.2019.05.020>.
- Combined Cycle Journal, (2012), "L-0 blade crack proves that although technical advisories age, they remain current", CCJ Online, Incorporated available at: <https://www.ccj-online.com/l-0-blade-crack-proves-that-although-technical-advisories-age-they-remain-current/> (Accessed: 11 May 2020)
- Duty, C.E., Drye, T. and Franc, A. (2015), “Material development for tooling applications using big area additive manufacturing (BAAM)”, *ORNL Technical Report ORNL/TM-2015/78*, available at: <https://doi.org/10.2172/1209207>.
- Duty, C.E., Kunc, V., Compton, B., Post, B., Erdman, D., Smith, R., Lind, R., et al. (2017a), “Structure and mechanical behavior of Big Area Additive Manufacturing (BAAM) materials”, *Rapid Prototyping Journal*, available at: <https://doi.org/10.1108/RPJ-12-2015-0183>.
- Duty, C.E., Kunc, V., Compton, B., Post, B., Erdman, D., Smith, R., Lind, R., et al. (2017b), “Structure and mechanical behavior of Big Area Additive Manufacturing (BAAM) materials”, *Rapid Prototyping Journal*, available at: <https://doi.org/10.1108/RPJ-12-2015-0183>.
- Fessler, J., Merz, R., Nickel, A., Prinz, F. and Weiss, L. (1996), “Laser deposition of metals for shape deposition manufacturing”, *Solid Freeform Fabrication Symposium Proceedings, University of Texas at Austin*.
- Flynn, J.M., Shokrani, A., Newman, S.T. and Dhokia, V. (2016), “Hybrid additive and subtractive machine tools - Research and industrial developments”, *International Journal of Machine Tools and Manufacture*, Vol. 101, pp. 79–101.
- Grujicic, M., Sellappan, V., Omar, M.A., Seyr, N., Obieglo, A., Erdmann, M. and Holzleitner, J. (2008), “An overview of the polymer-to-metal direct-adhesion hybrid technologies for load-bearing automotive components”, *Journal of Materials Processing Technology*, available at: <https://doi.org/10.1016/j.jmatprotec.2007.06.058>.
- Gupta, V. and Tandon, P. (2015), “Heterogeneous object modeling with material convolution surfaces”, *CAD Computer Aided Design*, available at: <https://doi.org/10.1016/j.cad.2014.12.005>.
- Hassen, A.A., Lindahl, J., Chen, X., Post, B., Love, L. and Kunc, V. (2016), “Additive manufacturing of composite tooling using high temperature thermoplastic materials”, *International SAMPE Technical Conference*.
- Hiller, J.D. and Lipson, H. (2009), “Multi material topological optimization of structures and mechanisms”, *Proceedings of the 11th Annual Genetic and Evolutionary Computation Conference, GECCO-2009*, available at: <https://doi.org/10.1145/1569901.1570105>.

- Islam, A., Hansen, H.N. and Bondo, M. (2010), "Experimental investigation of the factors influencing the polymer-polymer bond strength during two-component injection moulding", *International Journal of Advanced Manufacturing Technology*, available at: <https://doi.org/10.1007/s00170-009-2507-8>.
- Jeng, J.Y. and Lin, M.C. (2001), "Mold fabrication and modification using hybrid processes of selective laser cladding and milling", *Journal of Materials Processing Technology*, available at: [https://doi.org/10.1016/S0924-0136\(00\)00850-5](https://doi.org/10.1016/S0924-0136(00)00850-5).
- Jones, J.B. (2014), "The synergies of hybridizing CNC and additive manufacturing", *Technical Paper - Society of Manufacturing Engineers*.
- Kishore, V., Ajinjeru, C., Nycz, A., Post, B., Lindahl, J., Kunc, V. and Duty, C. (2017), "Infrared preheating to improve interlayer strength of big area additive manufacturing (BAAM) components", *Additive Manufacturing*, available at: <https://doi.org/10.1016/j.addma.2016.11.008>.
- Lauwers, B., Klocke, F., Klink, A., Tekkaya, A.E., Neugebauer, R. and McIntosh, D. (2014), "Hybrid processes in manufacturing", *CIRP Annals - Manufacturing Technology*, available at: <https://doi.org/10.1016/j.cirp.2014.05.003>.
- Liu, Z., Meyers, M.A., Zhang, Z. and Ritchie, R.O. (2017), "Functional gradients and heterogeneities in biological materials: Design principles, functions, and bioinspired applications", *Progress in Materials Science*, available at: <https://doi.org/10.1016/j.pmatsci.2017.04.013>.
- Lorenz, K.A., Jones, J.B., Wimpenny, D.I. and Jackson, M.R. (2014), "A Review of Hybrid Manufacturing", *Igarss 2014*, No. 1, pp. 1–5.
- Love, L.J. (2015), "Utility of Big Area Additive Manufacturing (BAAM) For The Rapid Manufacture of Customized Electric Vehicles", *United States*, available at: <https://doi.org/10.2172/1209199>.
- MacDonald, E. and Wicker, R. (2016), "Multiprocess 3D printing for increasing component functionality", *Science*, available at: <https://doi.org/10.1126/science.aaf2093>.
- Martinsen, K., Hu, S.J. and Carlson, B.E. (2015), "Joining of dissimilar materials", *CIRP Annals - Manufacturing Technology*, available at: <https://doi.org/10.1016/j.cirp.2015.05.006>.
- Sun, Q., Rizvi, G.M., Bellehumeur, C.T. and Gu, P. (2008), "Effect of processing conditions on the bonding quality of FDM polymer filaments", *Rapid Prototyping Journal*, available at: <https://doi.org/10.1108/13552540810862028>.
- Thermwood Corporation (2019), "Thermwood Introduces the LSAM MT", Available at: <https://youtu.be/yHLD4Bj0Me8> (Accessed: 11 May 2020).

- Turner, B.N. and Gold, S.A. (2015), “A review of melt extrusion additive manufacturing processes: II. Materials, dimensional accuracy, and surface roughness”, *Rapid Prototyping Journal*, available at:<https://doi.org/10.1108/RPJ-02-2013-0017>.
- Zhang, C., Chen, F., Huang, Z., Jia, M., Chen, G., Ye, Y., Lin, Y., et al. (2019), “Additive manufacturing of functionally graded materials: A review”, *Materials Science and Engineering A*, available at:<https://doi.org/10.1016/j.msea.2019.138209>.
- Zhu, Z., Dhokia, V.G., Nassehi, A. and Newman, S.T. (2013), “A review of hybrid manufacturing processes - State of the art and future perspectives”, *International Journal of Computer Integrated Manufacturing*, available at:<https://doi.org/10.1080/0951192X.2012.749530>.

CHAPTER 4. GENERAL CONCLUSIONS

This thesis presented a novel method for producing multiple material components consisting of metal and polymer regions using a hybrid additive and subtractive manufacturing approach. This objective was achieved through the execution of three studies:

- Evaluating performance and process parameters of a polymer AM tool incorporated into a machining center to create an in-envelope hybrid additive and subtractive system.
- Developing a method for creating a mechanically interlocking root structure for joining regions of dissimilar materials into a single component.
- Assessing the mechanical tensile strength of the root structure to understand the performance characteristics of the joint.

The work completed here to improve our understanding of how the cooling process parameters influence parts printed using the AMBIT PE-1 tool in a machining center can help guide other researchers developing large scale AM into hybrid systems. While thermal characteristics may differ from one system to another, this work can act as a guide for their efforts. Furthermore, this research demonstrated the importance of cooling on both the geometry produced and the resulting strength of the part. This research demonstrates the influence material flow rate has on porosity and the resulting part strength. These contributions further the understanding of large-scale polymer AM and helps enable its successful implementation.

This contribution expands the design space for components by increasing the number of materials that can be selectively specified to regions of component. Growing the possible material combinations allows designers to meet functional requirements by targeting material properties effectively. This process takes advantage of the synergies between additive

manufacturing and subtractive manufacturing processes by incorporating them in-envelope, allowing for each process to be used where advantageous. This combination allows for high productivity additive manufacturing through the use of high flowrate deposition while maintaining precision surface finish through subtractive manufacturing. Besides, the root structure allows for a tunable joint strength, allowing for break-away features to be produced. These features may be beneficial to incorporate sacrificial regions to prevent damage to more costly components or to prevent injury.

Going forward, there are some areas where more thorough studies can be conducted. A more in-depth investigation of the mechanical performance of the joint can be undertaken to understand how the root structure performs under different loading conditions. For example, loading conditions may include a peel style test, shear loading, and impact response of the part. Different polymers can be deposited into these root structures, and their performance should be better understood. For example, the filler material in the ABS polymer matrix can be modified, or the polymer itself could be changed. A dovetail cross-section for the root structure was investigated here, but there are other undercut features that could be implemented. Methods for nesting the root features into material transition cross-sections could be developed to automate this process planning step and to meet the strength requirements of a design.